Chapter 8

Architecture and Design Procedure of a Generic SWB Antenna with Superb Performances for Tactical Commands and Ubiquitous Communications

D. Tran, N. Haider, S. E. Valavan, I. E. Lager,
A. Szilagyi, O. Yarovyi and L. P. Ligthart

Additional information is available at the end of the chapter

http://dx.doi.org/10.5772/48487

1. Introduction

Ultra-wideband radio technology (UWB-RT) inherited a potential of extremely high rate of data communications, Claude Shannon discovered this in 1948 and derived the later-called-as Shannon-Hartley's channel capacity laws. This famous theoretical law however was not able to substantiate in practice until the development of the sampling oscilloscope by Hewlett-Packard in 1962, which, in accordance with the Nyquist-Shannon sampling theorem, was then capable to reconstruct at-that-time rather large UWB signals (Wilson, 2002).

UWB-RT, thus far, has been around for half a centuries but most research confined only in military applications and systems. The release of the 7.5 GHz of unlicensed spectrum by the US Federal Communications Commission (FCC, 2002) for commercial usages and applications in 2002 sparked a renewed interest in R&D of UWB-RT in industries, universities and governments. Today "ultra-wideband" usually refers UWB-RT where the electronic systems should be able to coexist with other electronic users (FCC, 2004).

UWB-RT and systems are becoming important not only to communications due to its high transmission capacity and speeds, but also gained strong foothold in many applications in the areas of industries, health monitoring, law-enforcement, defense and public security, etc.,.

Today, UWB-RT is not limited to carrier-free signaling but modulated in both analogue and digital domains typically in collision avoidance, medical imaging, security imaging

systems, through-wall, ground penetrating and LPI/LPD tactical command radar systems etc.,.

The UWB-RT has established indeed as an inevitable technology in the fabric of our everyday life, however, there remains significant number of challenges for the technology to become ubiquitous, especially in the safety and security issues. Enhanced by the decision on choosing mm-wave-based airport security passenger screening sensors by the Transportation Security Administration, new research directives in public security domain are the search for sensors with higher channel capacity, and screening with higher resolution. To compromise both range and Doppler resolution (Thor, 1962), Sensors which support super-wideband (SWB) signaling could be the solution for the problem at hand. Super-wideband radio technology (SWB-RT) could possibly be a potential approach enables high-resolution sensing in free space and in matter including ground-penetrating radar and through-wall sensing. SWB-RT has unique advantages as compared to narrowband technology, and also comprised all UWB-RT's advanced features but with more channel capacity, higher precision and super resolution in communication, ranging and screening, respectively.

The system's performance and characteristics are heavily dependent on the design of the radiating element. The requirements placed on UWB antennas in terms of *impedance bandwidth*, *size*, *phase linearity* and *spectral efficiency* are more demanding than for narrowband antennas (Valderas, 2011).

One of the challenges in the realization of SWB-RT is the development of a suitable antenna that sustains SWB-signaling. To obtain wider bandwidth, several bandwidth enhancement techniques have been studied such as: using log periodic arrays in which the different elements are deduced from an homothetic ratio (Rahim & Gardner, 2004), introducing a capacitive coupling between the radiating element and the ground plane (Rmili & Floc'h, 2008), using microstrip-line feed and notching the ground plane (Tourette et al., 2006), using symmetrical notch in the CPW-feeding (Zhang et al., 2009), asymmetrical feeding by micro-strip line together with reduced ground plane and appropriate gap-patch distance (Karoui et al., 2010), adding T-slots for both patch and feeding strip (Rahayu et al., 2008a), using cross-lot in the truncated circular patch with tapered micro-strip feed line (Kshetrimayum et al., 2008). All these techniques are based on the modification of the surface current distribution to broaden the antenna's impedance bandwidth.

We report here a *generic* SWB antenna architecture (SWBA), whose structure is purposely designed to support the functional section block division design approach (FSD, i.e. dividing the antenna structure into functional sections). The FSD in turn was utilized to accelerate the bandwidth optimization process; the SWBA and FSD together have conclusively enabled the designer to obtain antennas with SWB performances by optimization of just a few most-significant-parameters. It is noted here that in our SWB antenna, hereafter-named prototype 4, modifications were made not only at the feed-section but also the transition section and the radiation-section as well.

Anticipating and combining of all the advantages of its predecessors (prototypes 1, 2, 3), our new SWP-prototype 4 has been designed, fabricated and evaluated. Measurement results revealed that its SWP-performances are superior to other SWP-radiators reported in open-literature.

This chapter is organized as follow:

First, in §2 we discussed briefly the wire-version-antennas that all planar UWB and SWB antennas were derived thereof, the concepts of quasi-electric and quasi-magnetic for planar antennas are typically discussed, also definitions pertaining to qualitatively expressing the SWB antenna's impedance bandwidth were considered. In §3, the SWBA and the FSD are proposed and discussed. In §4, we briefly examine the performance of radiator prototype 1 as a "proof of concept" and provide a methodological procedure for simplifying the multivariate optimization (MVO) process, which were intensively used in the design of other prototypes 2, 3, 4, also parametric investigations and numerical simulations of the proposed SWB radiator are shown in this section. Technical issues related to the practical consideration of the design and fabrication are discussed in §5. Measurements of impedance bandwidth, reception patterns and pulse characteristics in both frequency- and time-domain are reported in §6. Acknowledgements are expressed in §7, and final conclusions are summarized in §8.

2. Fundamentals

In designing of cm-, mw-, and mm-wave antennas and components, comparing with the traditional wire- and waveguide-technologies, the planar technology offered numerous advantages such as planar, light weight, small volume, low profile, low cost, compatible with integrated- or with active-circuits, easy integrate into passive or active phased arrays and communication systems.

The planar technology facilitates the designers much flexibility in creating a myriad of different UWB and SWB antennas, the architectures of these antennas may different but their topology mainly resembles the traditional wire-version of monopole- or dipole-antennas. The nomenclatural names of planar antennas are confusingly taken over from the wire-version with similar topology. Topological similarities may support such borrowed name, nevertheless it is incorrect—as discussed in the next subsections—regarding to electromagnetic-properties point of view. To avoid such inconsistent idealizations new names and definitions, which support both topological and electromagnetic point of views, will be introduced in this section. We briefly start with recalling the traditional wire-version dipole and monopole antennas in §2.1, then the correct nomenclatures—for the planar-version magnetic and electric antennas—are introduced in §2.2, and end with their similarities: quasi-electric and quasi-magnetic antennas in §2.3

2.1. Dipole and monopole antennas

The Dipole antenna is one of the oldest radiators with theoretical expressions for the radiation fields being readily available (Balanis, 1997, p.135). The shapes of their radiation

patterns are also well-known [ibis., p.154]. The antenna first used by Hertz in his early RF experiments in the late 19th century, as an example, was a half-wave dipole (Krauss, op. cit.) and the shapes of its 3D-radiation pattern had a similar appearance to a full-doughnut or figure-eight (Balanis op. cit. p.163).

The Monopole antenna is formed by replacing one half of the dipole antenna with the ground plane, when the ground plane is large enough the monopole behaves like the dipole, except that its radiation pattern is just one half of the dipole, its gain approaches twice, while its length is one half of the dipole.

Magnetic dipole and electric dipole are standardized and well documented in [IEEE STD 145-1983, p.11-16]. The terms magnetic antenna and electric antenna were logically defined but occasionally used in literature, the first term used to describe radiators which possess radiation properties resembling those of thin wire loop (Balanis, op. cit., p.217), while the second is for those resembling of thin wire linear antennas.

2.2. Electric and magnetic antennas

Planar UWB and SWB antennas which geometrically resemble its counterpart (wire)-monopole antennas are widely called monopole. However, this topological naming for the planar radiators is incorrect and confused, because the radiation pattern of all the so-called (planar)-monopole antennas have not the shaped of the monopole but of the dipole antenna i.e., having the shape of the full-doughnut.

To avoid ambiguities, formal definitions for planar antennas are hereafter provided.

The definitions planar-magnetic antenna and planar-electric antenna were constructed by means of an analogy to the wire-loop antenna and the wire-electric dipole which are documented in (IEEE std, op. cit.; Schantz et al., 2003, 2004; and Tanyer et al. 2009a), to keep this chapter self-content and avoid cross-reference, we summarize them here:

As a first step, let the base plane B, be the plane comprises the antenna's effective radiating/ receiving aperture, and let $\mathbf{n}$ be the unit normal vector to this plane, with reference to Figure 5 , B can be assimilated into xOy, while $\mathrm{n} = \mathrm{i}_z$.

Assume that the field has a transverse electromagnetic (TEM) distribution propagating along the base plane. Then the following cases can be distinguished:

- In the case when the base plane magnetic field $\mathbf{H}(\mathbf{r})$, with $\mathrm{r} \in B$, is directed along $\mathbf{n}$, the radiator is referred as *magnetic antenna*.
- In the case when the base plane electric field $\mathbf{E}(\mathbf{r})$, with $\mathbf{r} \in B$, is directed along $\mathbf{n}$, the radiator is referred as *electric antenna*.

The above definitions are strictly applied to structures that support propagating-and-non-zero TEM- field distributions only, so that the waveguide case is automatically excluded by this TEM regard. We note here that the above definition have not taken in to account the diffraction effects at the edges/vertexes/corners of the metallic/dielectric material that constituent the transmitting/receiving aperture.

2.3. Quasi-electric and quasi-magnetic antennas

Most of the cases, particularly in planar antenna configuration, the topology of the radiating apertures may prevent the above-indicated conditions from being rigorously satisfied. Even in such cases, either one or the other of the two situations may prevail, thus correctly determine the type of the antenna. For instant, a radiator for which the magnetic field strength H(r) or the electric field strength **E**(**r**) is parallel to **n** over most of the effective aperture will be denoted as *quasi-magnetic* antenna, or *quasi-electric* antenna, respectively.

Obviously, planar antennas fed by microstrip-line or co-planar-waveguide can be classified as quasi-electric or quasi-magnetic antennas, respectively.

As will be demonstrated hereby, our prototypes fall in the class of quasi-magnetic antennas, whilst for all patch antennas fed by micro-strip line, as an example, the RAD-NAV antenna (Tran et al., 2010) belongs to the class of quasi-electric antennas.

2.4. Bandwidth definitions

There are several definitions of bandwidth circulated among our antennas and propagation society; those frequently met are octave-, decade-, ratio-, fractional-, percent-, and ratio-bandwidths. The two definitions, that most frequently used, are the percent bandwidth and the ratio bandwidth. They are defined respectively as follows:

$$BW_p \triangleq 100\% \times BW / f_c \tag{1}$$

$$BW \triangleq f_H - f_L \tag{2}$$

$$BW_{UWB} = \begin{cases} BW_{UWB,DARPA} \triangleq BW_p \geq 25\% \\ BW_{UWB,FCC} \quad \triangleq BW_p \geq 20\% \end{cases} \tag{3}$$

$$BW_{R:1} \triangleq BW / f_L, \text{ when } BW_p \geq 100\% \tag{4}$$

Where:
f_H, f_L are the maximum and minimum frequency at -10 dB, respectively.
BW is the nominal bandwidth defined by $BW = f_H - f_L$
f_C is the central frequency defined by $f_C = (f_H + f_L)/2$
B_P is the percent bandwidth and,
$BW_{R:1}$ is the *Ratio bandwidth*, commonly read as *R-over-1 bandwidth*, in which R is the normalized ratio of f_H to f_L defined as $R = f_H/f_L$, ($f_L \neq 0$)

The *percent bandwidth* (1) has originally been used to describe the narrow-bandwidth of conventional antennas and microwave-devices. Its usage is quite popular and often considered as a standard in many textbooks, nevertheless, it is mathematically not a solid definition because it possesses a defect when f_L approaching zero. For example, suppose that the nominal bandwidth of antennas #1 is 2GHz (0-2GHz), and antenna #2 is 20GHz (0-

20GHz). It is clearly that the nominal bandwidth *BW* of the second antenna is 10 times wider than the first one; however, formula (1) indicates that both antennas have the same percent bandwidth. Another weak point is the percent bandwidth of formula (1) is always less than or equal to 200% irrespective of how wide the antenna's nominal bandwidth was. Note also that formula (1) is often mistakenly called as *fractional bandwidth*, indeed the formula (1) consolidates its meaning "fractional bandwidth" only when the factor 100% is removed.

Alternatively, the *ratio bandwidth* (2) can also be used for expressing the bandwidth of UWB and SWB antennas and devices. The defect at zero- frequency point still lurks there but the 200%-limit is lifted. The use of the ratio bandwidth is more adequate to envision the wideband characteristics of devices under investigation. We choose for the second formula (2) for describing the bandwidth for the SWB-prototype discussed in this chapter.

How to choose two formulas, although no official consent however, the first formula is often used for cases that the bandwidths are less than 100%, whilst the second is for UWB and SWB antennas/devices.

Traditional communications systems typically used signals having a percent bandwidth of less than 1%, while standard CDMA has an approximately of 2%. Early definition in the radar and communications fields considered signals with percent bandwidth of 25% or greater (measured at the -3 dB points) to be ultra-wideband. The recent FCC regulations (FCC,2004), which will be used as a standard throughout this text, defined UWB devices/signals as having an nominal bandwidth which exceeds 500 MHz or percent bandwidth of over 20%, measured at -10 dB points.

The term SWB has been often used to indicate bandwidth, which is greater than a decade bandwidth. Since the percent bandwidth confused and failed to envision the SWB property adequately as discussed in §2.4, the "ratio bandwidth" is more suitable and often be used for describing bandwidth of 10:1 or larger, we adopt this convention throughout this report.

The proposed antenna possesses

3. UWB/SWB antennas, a review

3.1. Planar dipole antennas

Common and most-used planar dipole antennas are shown in **Figure 1**. They are well-known for their enormous impedance bandwidth (**Figure 2**), and have been used in many applications. However, their radiated/reception patterns, as shown in **Figure 1**, are not stable/usable in the whole of their claimed bandwidth, so the naming "*UWB/SWB*" may be argued, and the needs for true UWB/SWB antennas which consolidate their name in not only impedance-bandwidth, but also in other criteria as important as radiation patterns, gain, phase, group delay, etc.,. The pattern distortions have been studied and clearly pointed out by many several researchers, excellent research-works on this topic are reported, we cataloged here only some of the most pronounced works, to name a few, Marsey(2007), Biscontini(2006), Hayed(2007), Chavka(2006), Ruengwaree(2007), Garbaruk(2008), Welch

(2002). Close inspection the patterns displayed in fig. 1 (and in all referenced work above) we discovered a **remarkable** general property that pattern dispersion became lesser as the antenna's sharp corners becoming more rounded. So our generic radiator

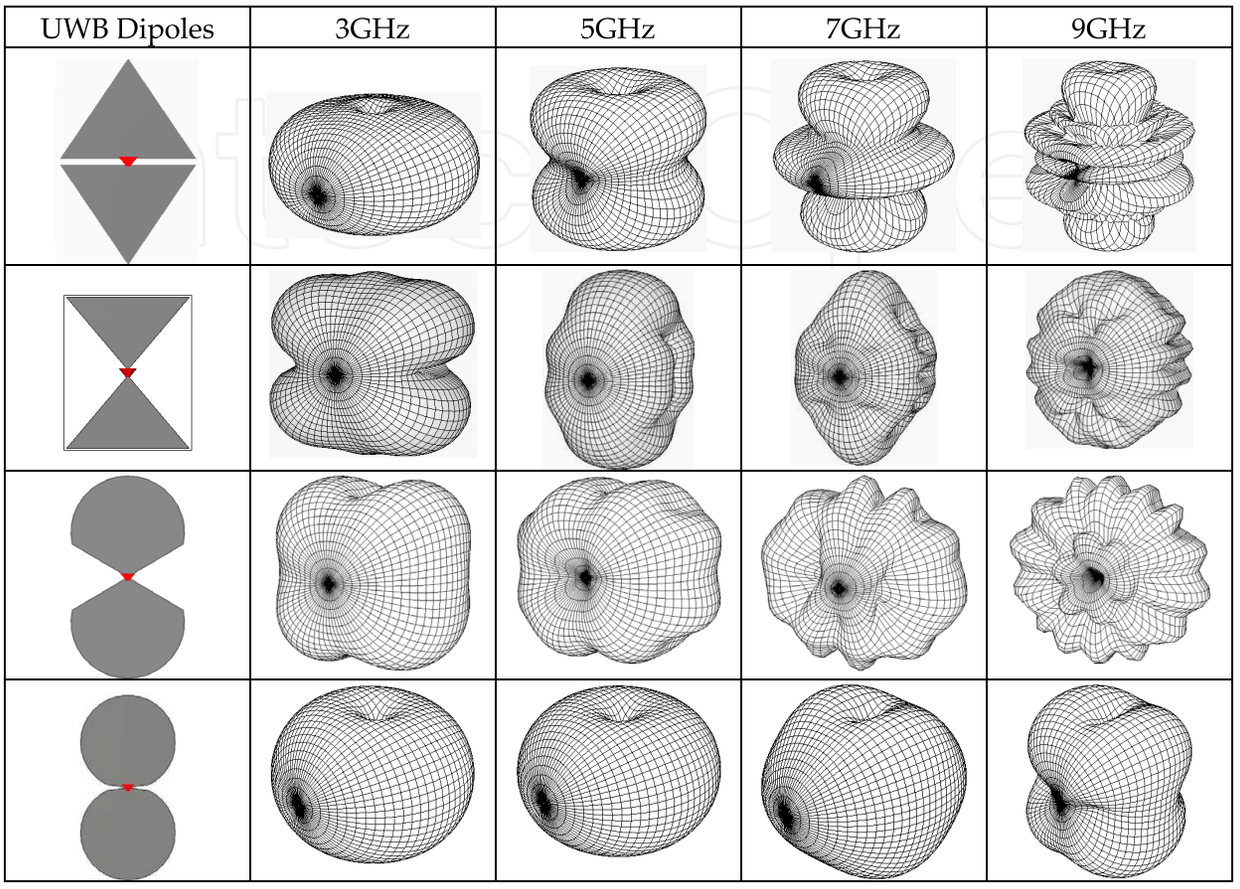

Figure 1. Distortion of radiation patterns of common planar UWB/SWB radiators

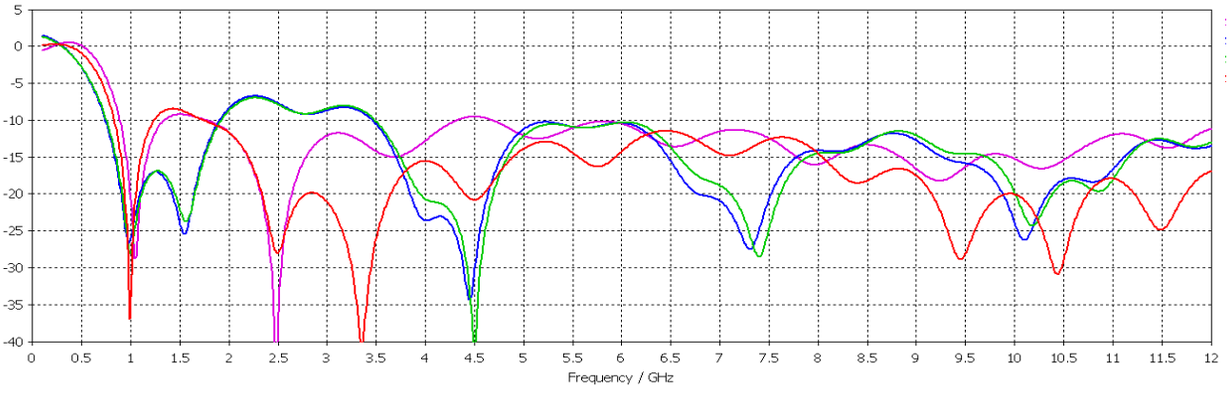

Figure 2. Typical extremely large impedance bandwidth of planar dipole antennas

3.2. Planar monopole antennas

There are countless numbers of UWB/SWB monopole antennas have been developed in the last 20 years, the variety in shapes and architectures vary enormous. **Figure 3** represents the

most important monopoles which have been already designed, patented and published in both open and close literature.

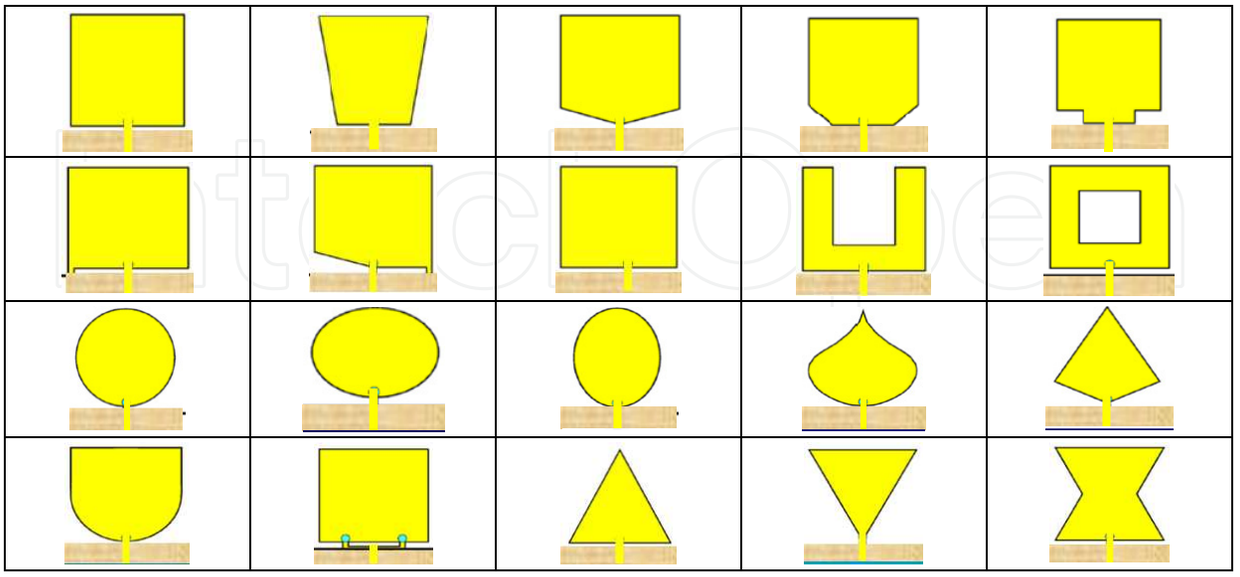

Figure 3. Monopole planar antennas(Courtesy of Dr. S.W Su, Department of EE, NSYSU)

3.3. Antenna miniaturization

The bandwidth and geometrical dimensions have been remarkably reduced, best achievements are timely listed in Table 1, for the used miniaturized concepts and techniques, the readers please consult the references in the listed table.

Antenna	Feeding	Dimension~	Bandwidth	Created by
Slot	Coax-CPW	130x130 mm^2	0.5-7 GHz	Yeo, et al., 2004
Monopole	CPW	70x70 mm2	1.5-3 GHz	Chiou et,al, 2003
Pulson 200	Microstrip	40x80 mm^2	2.5-6 GHz	Schantz, Time Domain. 2003
Elliptical slot	Coax-CPW	55x50 mm2	3-12 GHz	Ying et al., 2004
Square monopole	Microstrip	50 x50 mm^2	3-11 GHz	Battler, M. et all,2006
Monopole	Microstrip	30x40 mm2	2-12 GHz	Xiao et.al., 2009
Monopole	CPW	30x40 mm2	3-12 GHz	Shastry et al., 2009
Elliptical slot	differential	27x46 mm2	3-12 GHz	Power et al., 2004
Vivaldi	Microstrip	35x35 mm^2	1-12 GHz	Abbosh et al., 2007
Monopole	Microstrip	30x35 mm^2	3-12 GHz	Choi et.al., 2004
Monopole	Microstrip	30x33mm2	3-11 GHz	Kimouche et al., 2009
Monopole	Microstrip	30x32 mm2	2.9-13.2 GHz	Choi et.al., 2009
Monopole	Microstrip	30x30 mm2	3-11 GHz	Rahayu et al., 2008b
Monopole	Microstrip	25x25 mm^2	3.2-12 GHz	Cho et al. 2006
Generic	CPW	15x15 mm^2	5-150 GHz	This work

Table 1. Most pronounced UWB/SWB monopole antennas

4. Antenna topology, architecture and the FSD methodology

Since the release of the license-free band and the regulation of the emission spectra by the FCC in 2002, a myriad of UWB antennas have been created and invented by both industry and academia, most of them are limited to the FCC-band, this 7.5GHz bandwidth corresponds to a moderate short pulse in order of nanoseconds, these short pulses are good enough for high capacity communication, accurate ranging and imaging but not enough for the more stringent needs of precise localization, high resolution screening, sensitive sensing. To satisfy such stringent requirements, challenges are placed on the design of sensors that support signaling of extreme short pulse in the order of hundreds of picoseconds or less. Sensors in the terahertz region support such short pulse and unarguably provide sharpest images, nonetheless the detection range is too short and the sensors are very costly. Note that in the terahertz region, a radiator with only 5% is capable to support , for example, a Gaussian pulse of 20 ps (assumed unity time bandwidth product), while in the RF-region one must have a SWB radiator of over 11:1 (or 167%, by a lowest frequency of 5GHz) for signaling such a short pulse.

There existed broadside and end-fire UWB antennas with different topologies, which comprised of many configurations are available in open literature. The pattern stability of several antenna's topologies and architectures had been thoroughly investigated and reported by (Massey, 2007, p.163-196). It seemed that there was no broadside antenna architecture could exhibit stable patterns within a bandwidth wider than 10 GHz, and most of them are UWB-radiators with ratio bandwidth much less than 10:1.

We propose here an SWB antenna architecture which possessed not only SWB bandwidth lager than 10:1 but also exhibited a much stable patterns in its SWB bandwidth than all those which have been studied and reviewed by (Massey, op. cit.). The SWB prototype 4, and all other prototypes reported in this chapter had been designed, fabricated and evaluated at our IRCTR.

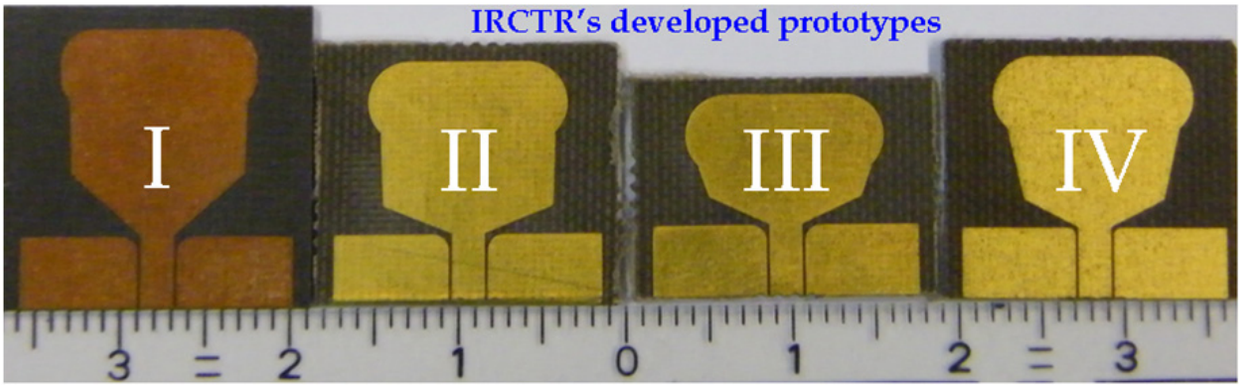

Figure 4. Prototypes developed at IRCTR, resulted design dimensions are listed in table 2.

The SWB radiator reports in this chapter, was indeed a revolutionary improved version from IRCTR's previous developed prototypes. All the developed prototypes, shown together in Figure 4, shared the same topology and architecture as depicted in Figure 5a.

The kernel of this topology is its simplicity, and the essence of the antenna's architecture is the logicalness of dividing the antenna into functional section blocks that enables simplifying the MVO process into a sequence of single-variable optimization (SVO) one.

Simplicity: the topology of the proposed antenna is simple in design with just a copper pattern on top of dielectric layer, the employment of dielectric layer is just for the purpose of structural rigidity of the prototype. In fact, without the dielectric layer, the propose antenna performs much better in terms of matching, and having more perfect symmetric and stable patterns and lower cross-polarization.

Compactness: Thank to the functional section block design (FSD, to be discussed in next section), we are able to miniaturize the generic antenna in an area as small as 15x15mm^2, Table 2 shows comparative indication of miniaturization effectiveness of different proposed architectures.

The merits of the topology, architecture and logical functional blocks, and optimization process will be discussed in §4.1, 4.2 and 4.3, respectively.

The original antenna topology and architecture of prototype 1 leaved many flexible possibilities for adjusting parameters or scaling dimensions to meet new requirements or applications without much entangled in complicated MVO process. These possibilities have been exploited to double the antenna's bandwidth of prototype 1 (Tran et al, 2007) from 2:1 to 4:1 by (Tanyer et al., 2009a), and further broaden to 9:1 (Tanyer et al., 2009b), and scaled down to the FCC-band for IR-applications (Tanyer et al., 2010).

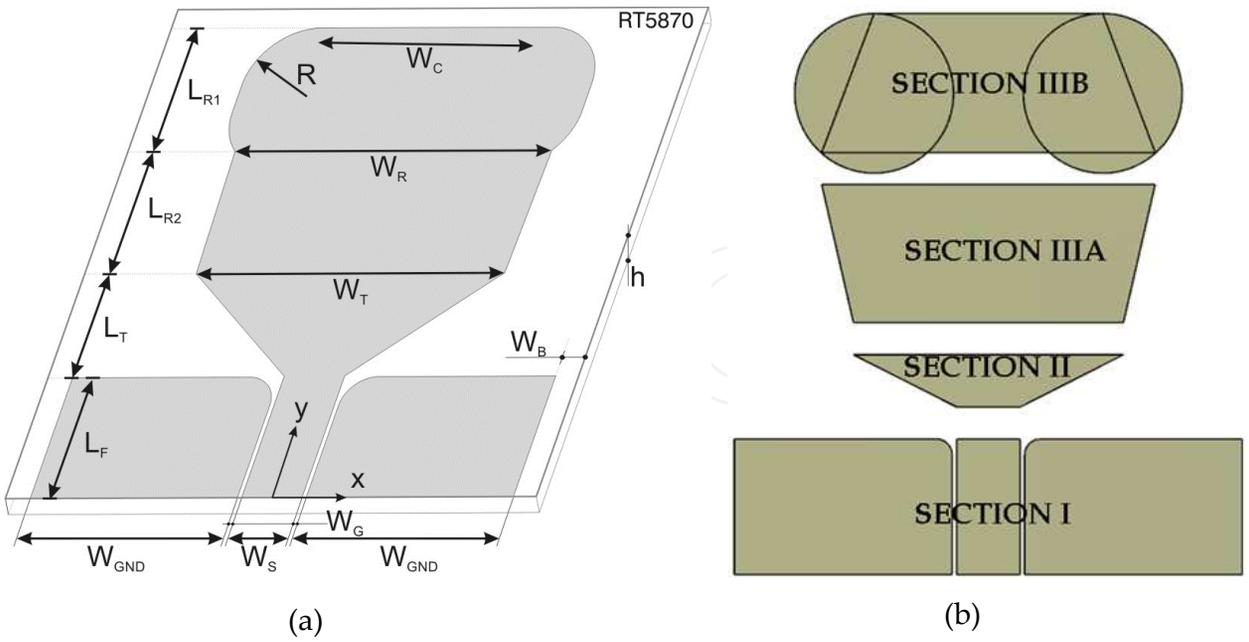

Figure 5. Proposed configuration: a) Architecture and parameters, b) logical functional sections.

The prototype 4 is a proof of concept in proving viability of the design of radiators, which are capable of supporting such extreme short-pulse in RF/mmw-region. The proposed

antenna's topology, architecture and the FSD approach, as will be discussed in subsequence sections, were objectively aimed at two main goals:

- Choosing an antenna topology whose shape is kept simple regarding ease of fabrication, prevent diffractions, easy to scale up/down to meet designer's requirements in size and performance (§4.1).
- Creating an architecture that providing a basis platform for implementing the "FSD approach", and deploying the conceptual "thumb-rules" for effective simplifying the MVO process in to SVO, a much simpler one (§4.2).

4.1. Antenna topology

The starting point in the design of the SWB antenna reports in this section is mainly credited to the original radiator (Tran et al., op. cit.), whose topology is planar, as sketched in Fig.5a, with structural topology comprised of following stack-ups:

- Single dielectric layer to provide structural rigidity.
- CPW feeding structure on top of the structure.
- An antenna patch is directly connected to the CPW-feeding, so that they together formed a single planar pattern run on top of the structure.

The CPW feeding structure has been chosen because of it well-behaved properties: such as negligible radiation, low loss, the effective dielectric is constant over a sustained wide frequency range, where the later property is more suitable for super-wide-band feeding a SWB-radiator than the micro-strip line (Simons, 2001).

4.2. Antenna architecture and the FSD approach

In antenna design if dimensions are unconstrained and by a proper design, antenna will behave as a high pass filter, and if its dimensions are physically large enough then all frequencies will pass through. Research of published papers over UWB and SWB antennas reveals that most of the UWB and SWB antennas had a considerable larger size, mostly lager than $\lambda_L/2$ of the lowest frequency f_L, and on broadening the bandwidth, a first option, was to resort to stochastic optimization methods, nevertheless, these methods are known for carrying extremely high computational load.

A more feasible alternative approach was provided by the critical analysis of the relationship between the geometrical parameters and the physics of the problem at hand.

The FSD approach was intentionally created in such a way that the overall dimensions are constrained, kept small and the process of optimization can also be simplified.

The logical architecture together with its parameters and FSD are sketched in Figure 5a&b.

The FSD approach follows the bottom-up strategy, i.e.:

- Starting from the *feed section*—its CPW feed supports the required impedance bandwidth for SWB signaling.

- Then to the *internal transition section*—this section is intentionally inserted between the feed and the patch for the purpose of impedance matching, its shape was logically chosen so that it able to serve the design-properties: resonance shifting, impedance matching, and also enable parameter to serve as independent optimized parameter.
- In addition to the *radiating section*, we divided it in to two sub-sections, which are the *patch section* and the *external transition*. The patch section creates an extra degree of freedom to ease the optimization process, and the radiating section provides parameter for shaping radiation patterns. Two round areas had been added to the top corners of the patch for the purpose of 1) diminishing of diffraction at the antenna's top vertices (deformation of sharp corner in to circular edge) and, 2) controlling and retaining the shaped of the radiation patterns at high frequency band of the spectrum, and, 3) subduing the number of parameters to accelerate the optimization process. These four sections are orderly numerated as I, II, IIIA, and IIIB in Figure 5b.

In summary, the FSD approach assumed the following steps:

- Keep the antenna's overall dimension small and fixed;
- Start orderly from section I, II, IIIA and IIIB (this bottom-up strategy prefers matching impedance bandwidth in prior of pattern bandwidth);
- Separate and understand the role of each section;
- Identify the parameters associate with that section, select the parameter that predominantly influences the function of that section.
- Isolate the effect of that parameter so that an optimization only on that parameter can be undergone, without affecting too much the performance of other sections.

Based on the FSD approach the prototype 1 was first designed and evaluated (Tran et al. 2007). Its designed parameters are used as *start values* for the optimization process of all the later prototypes. Four prototypes (1, 2, 3, 4 shown in fig.4) were successful designed and evaluated, the prototype 4 proved to be a radiator which is superior to the others in that both of its impedance bandwidth and radiation pattern are SWB-sustainable.

4.3. Generic architecture

With the proposed antenna topology and FSD-architectures, we obtained a generic configuration that can be used as a configurative template for finding the perfect antenna configuration (shape + dimension) which fulfills the constraints place on sizes, bandwidth, and dispersion (pattern, gain flatness, linear phase).

Figure 6 shown typically some of the many possible UWB/SWB antenna configurations, which are all generated by varying just some of the design parameters of the same original generic architecture, proposed in Figure 5. Note that all of these antennas are UWB/SWB, and although they are subsets of the generic configuration, but only one third of them worth to be called UWB/SWB antennas when their usable UWB/SWB patterns are considered. It is worthy to note that the antennas (2, 3, 4, 5, 6, 7, 9, 10, 11, 13) generated by our generic architecture have been intended/published/patented by other researchers several years ago.

Our generic architecture generalized, showed the connections between them, and proved that they are just particular cases of the introduced architecture.

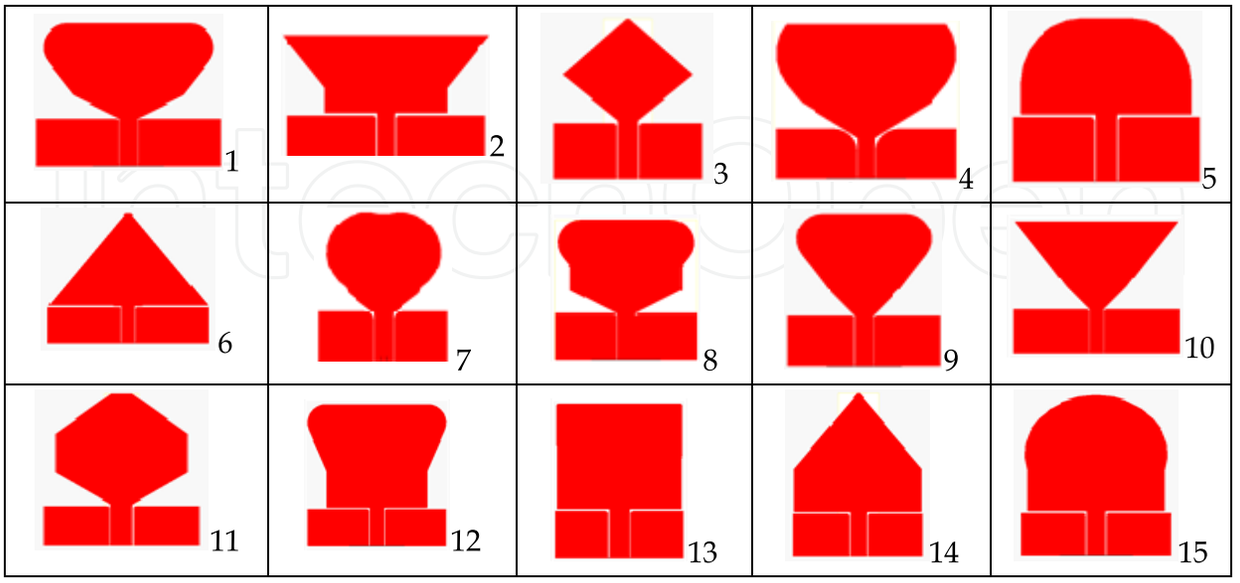

Figure 6. Proposed configuration: a) Architecture and parameters, b) logical functional sections.

4.4. Parameter identification and optimizations

Prototype 1: elaborated by (Tran et al. op. cit.), formed a basis for the designs of the later prototypes. Its 10GHz impedance bandwidth and designed parameters are plotted in fig.9 and listed in table 2, respectively. For the detailed works and the measurement results, the reader should refer to (Tran et al., op. cit). The other prototypes all took the designed parameters of prototype 1 as start-values, and used the FSD to identify the significant parameter for its SVO process of bandwidth broadening.

Prototype 2: is obtained by taking the start values of the prototype 1, and using FSD to identify the LT as its significant parameter for SVO process. The resulting designed parameters and the impedance bandwidth are listed in 2nd column of table 2, and Fig.9, respectively. The SVO demonstrated the solidity of the FSD approach that the bandwidth can be doubled (from 10GH to 20 GHz) by optimization of just a single parameter LT. For details of the elaborated work, please refer to (Tanyer et al., 2009a, op cit.)

Prototype 3: by keeping LT fixed, the prototype 3 is obtained by optimizing the lower part of the radiation section which comprised of two parameters LR2 and WT, the first make the total length of the radiator shorter (thus affects the higher frequency), whist the second parameter provide an better match (i.e., lower reflection coefficient). By doing two SVO sequentially (first with parameters LR2, then WT) we again doubled the nominal BW (form 20GHz to 45GHz), in term of ratio bandwidth it is of BR = 9:1 as shown in Fig. 10. The resulting parameters are listed in column 3rd table 2. Further details of measurements and other properties of this prototype 3, are detailed in (Tanyer et al., 2009b, op. cit).

Prototype 4: is obtained by the combined optimization of the FSD-identified parameters WT and WC, By keeping the optimized parameters of the previous optimization steps (LT of prototype 3, all others of prototype 1) fixed, and doing 2 SVO sequences, we obtain the SWB impedance bandwidth of BR greater than 30:1, the result is plotted in Figure 9, the corresponding design parameters are listed in table 2. We noted here that by controlling radii-separation distance WC we are able to keep the radiation pattern of this prototype less distorted till 50GHz as shown in Figure 8.

The created parameters, their functions, their effects and their usages are discussed in greater details in the next sub-sections. The FSD is detailed in §4.5-4.7, the resulted SWB-performances are given in §4.8 and in §4.9, the optimizations of all the prototypes are discussed in details.

4.5. Section I: The feed section

Planar antennas and arrays have been used for micro-wave and millimeter-wave applications for decades, especially in mobile communications where system design requires low profile, lightweight, and high directivity. The two most used feeding methods are micro-strip line (MS) and coplanar waveguide (CPW), they both carried signal excellently in narrow-band and UWB antennas and devices. Many planar antenna arrays have been designed by using MS, however, until recently, only a few works so far have used CPW to feed the array. The CPW has gained increasing popularity in recent years, since it has several advantages over the MS, such as low radiation losses, less dispersion, easier integration with solid-state active devices, and the possibility of connecting series and shunt elements, and suitable for SMD-technology, also for SWB- antennas/devices CPW feeding provides better match and performs better than the MS line (Simons, 2001).

In search for the SWB radiator, both radiator and the feed must be super wide band. Since the SWB-signal first must able to pass through the feeding-line before reaching the antenna, obviously that the feed must be considered first in advance of other sections, we conduct the work with bottom-up approach, i.e., the feed is consider first, because if the feeding mechanism fail to be SWB, then there is no SWB radiator exists no matter how good the radiator will be. The coplanar waveguide is the first choice for feeding the signal to the radiator, because the CPW's effective dielectric is constant, (this property is a key feature in wide band matching the antenna), over a wider BW than micro-strip line, another advantage is, in contrast with MS line, one of the parameter pair (WS, WG) can be varied in size and shape, whilst the other is correspondingly changes to keep the characteristic impedance stays unchanged, furthermore CPW is low-loss, and the signal width can be chosen width enough to support characteristic impedance from 30Ohm and higher (Simons, 2001, p.52),

The CPW would be a better choice for SWB-feeding because of it considered features, summarized as follows:

- **SWB behavior**: the effective dielectric constant is almost independent of frequency (Simon op cit.), this feature is a priori condition for SWB feeding and matching.

- **Dimensional flexibility**: the width of the signal line, and hence the corresponding gaps, can be freely designed to accordingly support the physical dimension of the transition region and the antenna.
- **Dielectric support**: The dielectric thickness exerts negligible weight on the economy of the CPW-impedance

4.6. Section II: The tapered transition

The tapered transition has been inserted between the CPW-feed and the radiating patch, this section responsible for a smooth transition between the feed and the antenna, and because the current distribution is denser in this region than the others, this property indicated that this section must have strongest influence in matching the impedance bandwidth. This section has two parameters (LT, WT), which are described in details in §4.6.1 and §4.6.2 below.

4.6.1. The internal Transition Length LT

The length LT of the tapered transition (section II) is responsible for the smooth transition between the feed and antenna, and proved to be the most sensitive parameter in the design of our prototypes. Anticipation from the theory and design of micro-strip antenna (MSA), it is well-known that the length of the MSA determines the resonance frequency (by lengthen or shorten this parameter, one can shift the resonance frequency to lower or higher band, respectively).

The antenna's resonance is affected by its length, this length is composed by LT + LR1 + LR2, when this composed length is changed, and the resonance will presumably change accordingly.

It is observed, from the results plotted in Fig.9, that when LT is longer the resonance will shift to lower frequency (as shown by prototype 1, LT = 3.64, Fig.9), and when LT is shorter the radiator's resonance will shift to higher frequency (prototype 2, LT= 1.64, Fig.9)

4.6.2. The internal Transition Width WT

The width WT of the taper transition section (section II), is also a "share-parameter" with lower radiating section (section IIIA); this width provides, as similar role as the width in microstrip patch antenna, a fine-tune mechanism for impedance matching as its nominal value varies. This enhanced matching mechanism are numerically demonstrated with the reflection coefficients of the prototypes 3 and 4 as plotted in Fig. 10, in which they shown a lower reflection coefficient, i.e., a better match.

4.7. Section III: The radiation section

This section comprise of six parameters LR1, LR2, WT, WR, WC, and RC, in which WT is the share parameter described in §4.6.2, we divided this section into sub-sections IIA and IIB

as sectioned in Fig. 5b. The parameter set of the internal sub-section (IIIA) and the external parameter sub-section (IIIB) are {WT, WR, LR2} and {WR, LR1, WC, RC}, respectively.

4.7.1. The internal radiating matching section

Two parameters, which identified to be key player for this subsection, are {WT, LR2} (the WR is not touched because it is share parameter of these two sub-sections), by first optimize the width parameter WT, and by keeping this optimized parameter fixed, and continuing to optimize the other parameter LR2. By this token, (Tanyer et al., 2009b, op cit.) obtained a huge enhancement in ratio bandwidth reported as 9:1. The design parameters are listed in table.1, the result is plotted in Fig.9. More detailed works and measurement results, the reader should refer to (Tanyer et al., op cit.).

4.7.2. The external radiating transition section

This sub-section was often neglected by the designers due to the fact that the current distribution is weak along the edges of this section. However, we observed that it plays an important role in maintaining the shape of radiation pattern in a wide range of frequencies, as will be numerically proved in §4.8

The sub-section IIIB consists of a set of parameters {WR, LR1, WC, RC}; WR is a share parameter so we keep it intact. From fig.1 it is seen that WR1 is suppressed and covered by varying the radii-distance WC, we can also single LR1 out because it contribution to the length of the radiator can already be economized by LT and LR2, so WC is the only parameter left that we may use to fine-tune the radiator for both SWB performance and radiation pattern characteristics. Prototype 4 utilized this philosophy by varying LR2 (instead of LR1) and WC to obtain the super wideband performance plotted in Fig.7. It is observed that variation of WC had no significant impact on reflection coefficient (current distribution along the antenna circle edges are rather week compared with those close to the tapering transition region). Nevertheless, by properly controlling WC we are able to maintain the usable shape of the radiation patterns up to 50 GHz as shown in Fig.8. So, WC is clearly to be the parameter to control the interference of the edge/corner scattering and diffraction of the radiator. In transforming the vertex-diffraction to edge-diffraction, we advocate the use of circular shape; nevertheless, other researchers suggested the shapes (elliptical, football cape, etc.). To answer the question which shape would serve best, we need a further in depth study about all possible pattern sensitive shapes before providing a final conclusive appraisal.

4.8. The prototype 4 and its super wide band performances

Fig. 7 shows the simulated result of the magnitude of the reflection coefficient of our SWB prototype 4. We computed and shown here only up to 150GHz. By close inspection of the reflection coefficient, the reader could observe that the prototype 4 shows a trend and exhibits the behavior of an all-high-pass antenna; its impedance bandwidth could be much wider than shown here.

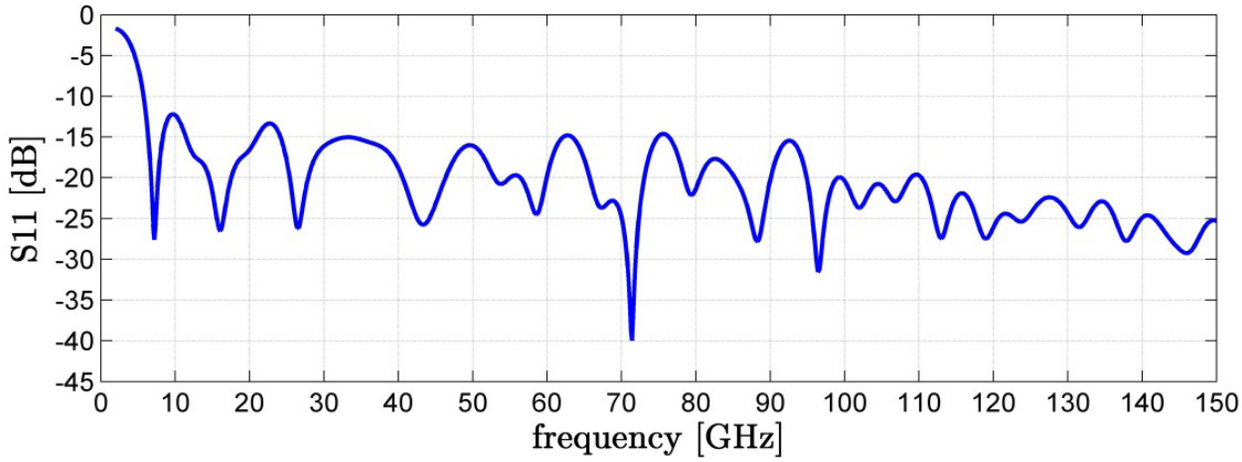

Figure 7. Impedance bandwidth performance of the proposed prototype 4.

The numerical results were computed with the following practical assumptions:

- The relative dielectric constant and the loss are assumed constant over the computational bandwidth.
- The commercial Duroid RT5870 high frequency laminated material we used, in deed could practically support up to 77 GHz only (Huang, 2008, p.64); beyond this frequency we may have to look for other dielectric material.

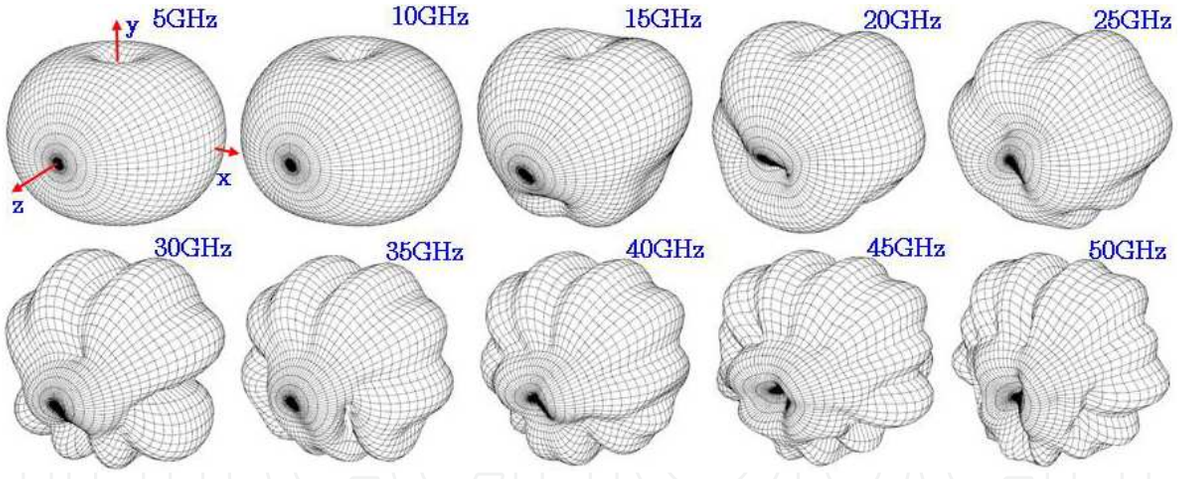

Figure 8. Pattern performance of prototype 4. Complete spectra of 3D-farfield co-polar radiation patterns from 5 to 50 GHz with increment step of 5GHz.

Fig.8 shows the simulated 3D radiation patterns of prototypes 4; the plot indicated that the radiator exhibits a super wide band pattern characteristics, the usable spherical patterns are sustained in a bandwidth wider than 10:1. The SWB properties displayed in fig.7 and fig.8 shown that prototype 4 is a true SWB radiator in both impedance and patterns aspects, and its SWB-behavior is superior to antennas reviewed by (Massey, 2007, pp.163-196). We emphasize here that this radiator is termed as quasi-magnetic antenna, because it is clearly seen that this antenna possessed radiation patterns similar to that of a dipole, therefore calling it monopole reflects wrongly the EM-characteristics that it possesses and exhibits.

4.9. Optimization process and development of prototypes

Although the proposed topology and architecture is simple, however with a total of 14 parameters it would be an impossible task for the multivariate optimization process.

This section reports in details of how to delimit the variables and how to reduce the number of variables for simplifying the MVO process to a SVO one. In addition, some pragmatic rules are also given for identifying the key parameters, and for weighting the priority of those parameters in the sequentially SVO processes.

To keep the optimization process controllable en less entangled in multivariate-optimization process, efforts have been done in the following steps:

Step 1. Topology and architecture: this step is important in that it had to form a basis for the FSD, and had to keep the antenna topology as simple as possible, but not simplest as (Al Sharkawy et al., 2004), Although all efforts has been carried out to ensure a minimum amount of the created parameters, the structure (fig.1a) still have a considerable set of parameters { ε_r, h, t; L_F, W_S, W_{GND}, W_G; L_T, W_T; L_{R2}, W_R; L_{R1}, W_C, R }.

Step 2. The FSD: dividing the radiator into sections depending on their main function. Inspection of the radiator's current distribution and the radiator's topology shown in fig. 1a revealed that the radiator could presumably be divided into functional sections as depicted in fig. 1b. The analyzing and optimizing process are conducted following the bottom-up approach that always started from the feed (section I) and ended at the last radiation-section (section III.B). The analysis, optimization and development of the prototypes all should start and avoid as much as possible the *share-parameters* between sections (W_T , W_R); if impasse is met then, as a thumb-rule, the section on top has priority on taking the share parameter.

Step 3. Excluding of fixed parameters: The numbers of parameters of the radiator have been reduced by singling out the non-optimizable parameters. The first three material-parameters { ε_r, h, t}, because their nominal values were already fixed by the manufacturers, are not quite suitable for optimization process as continuous-parameters, so the parameters of the feed section (section I) are kept fixed and excluded in the optimization process.

Step 4. Setting boundaries: in order to accelerate the optimization process and avoiding the problem of unbounded optimization, we put geometrical restrictions on the total width (2WGND + 2WG + WS) and length (LF + LT + LR2 + LR1) of the antennas fixed to λb/2, where λb is wavelength at the design-frequency, and force all the internal parameters and their combination to be constrained inside this antenna's boundary λb/2.

Step 5. Reduction of parameters: in this step, we did further reduction of the number of parameters involved. Exploiting the fact that the feed-section's parameters have no significant added values to the total performance once its optimum values are founded, and the following prior measures have been set, 1) for impedance-matching it is fixedly set to 50 Ω and, 2) for field-matching the impedance-parameter-pair (WS, WG) has been chosen such that it is wide enough to support the currents to separately flow along the edges of the signal line WS, and the feed length LF must be long enough to support the

transformation from coax's TEM to quasi-TEM of the CPW line, so the feed's parameters can ruled out for optimization, and set to be fixed with values as listed in table.1.

Step 6. Start values: This step initiated the start values for the set of parameter listed in step 1. The initialization of the start values was elaborately detailed in (Tran et al., 2007). Prototype 1 (Fig.4) with the start values as listed in table.1, obtained a BW of 10GHz (fig.9). Detailed discussions and simulated, measured results can be found in (Tran et al., op. cit.).

Step 7. Simplified process: The 7th step is the simplification of the optimization process by breaking the MVO process down into series of SVO one. It was observed that the current intensity is mainly distributed along the edges of the transition region, this suggested that : a) small variation of the transition parameter in this section (LT, WT) would have a strong influence on the flow of the signal current and hence play a large impact on the impedance bandwidth, and exploiting the fact, as similarly in microstrip antenna, that b) the length of the radiator defines the shifting-property of the resonance, whilst c) the width of the radiator effectuates the matching-property, and d) another independent-property is that they can be separately optimized.

So by keeping WT, the share-parameter between sections II and III.A (fig.5b), fixed and took just a single-variable-optimization (LT), the impedance bandwidth was double to 20GHz as obtained by prototype 2, which is plotted in fig.9. The parameters of prototype 2 are listed in table.2, more details of the electromagnetic properties and measurements regarding the performances of this prototype can be found in (Tanyer et al., op. cit.).

Step 8. BW enhancement: Prototype 3 (fig.4) was obtained by analyzing and optimization the lower part of radiation section IIIA (fig.1b). This section has three parameters (WT, LR2, WR); first, following the rules discussed in step 2 we left out the parameter WR since it is the share-parameter between section IIIA and IIIB; next, in order to avoid multivariate-optimization, anticipating the shifting-property and matching-properties discussed as (b) and (c), respectively, in step 7; then two SVO sweepings were carried out, first WT (property c) and then LR1(property b); the order of WT or LR1 can be chosen freely according to independent-property (d, in step 7). The design parameters of prototype 3 are listed in table.1 in which the parameters of the previous optimized prototype are kept fixed, only the two parameters (WT and LR1) belonged to section IIIA are investigated and optimized.

Step 9. The design of prototype 4 is aimed at two SWB-compliances: 1) SWB impedance bandwidth, and 2) SWB radiation pattern. The radiation section consists of the following set of parameters (WT; LR2, WR; LR1, WC, R), the length parameters of this set can be keep fixed, because LR2 and LR1 are resonance-shifting parameters, and the antenna architecture allows us to use other length of the antenna to control the resonance, this was already done by LT of the lower section, so these two parameters can be singled out of the optimization process; the share parameter WR can also be neglected because it matching-property is covered by the set {WC, R}, so by keeping R fixed the parameter set of section III was left with only two parameters left {WC, WT}. The procedure followed: fist, keeping the parameters of prototype 1 with the optimized

LT = 1.64mm, then two SVOs were carried out first for WT and then WC. The reason that WT was chosen first is twofold, 1) WT is more sensitive on matching because the current distribution is denser at the lower part, 2) WC is the share parameter that mainly located in section IIIA where the matching effect is week, and it is purposely inserted to control the radiation patterns instead of wideband matching the radiator. The optimized parameters of prototype 4 are listed in table.2. The impedance bandwidth of the prototype 4 is plotted in fig.9, and fig.7; also, its SWB radiation patterns were in fig.8.

Prototypes 1, 2, 3, 4 have been design, fabricated, measured and evaluated, photographs of them are shown in fig 4. At first sign, they seemingly looked different, however they all shared the same topology and architecture as depicted in fig.5a, only one or two parameters is slightly changed to obtained difference desired performances. For comparison, their correspond impedance bandwidths are plotted together in fig.9. The impedance bandwidth enhancement is improved from 10 GHz, to 20 GHz, 40 GHz and beyond 150 GHz as shown in fig.9 and fig.7

4.10. Comparison of the prototypes

The design parameters of prototype 4 and all other prototypes are listed in table.2, so that, the reader, could independently recheck, or reproduce them without much difficulty.

These are results of the FSD methodology and SVO steps described in previous sub-section (§4.9). Note that the SVO should be carried out orderly by A, B and C. (bold and capitalized in table.2), A is dedicated as the first to be optimized, keep that optimized parameter fixed, and goes on with B, then continue with C. For example, the prototype 4, (A) first fixing the taper's height LR2 to 4.335mm, then (B) optimizing the taper width WT, and then (C) adjust the WC for the radiation-characteristics. The optimized results showed an SWB impedance bandwidth of at least over 150GHz. In fact the result of prototype 4 (with parameters listed in column 4 of Table.2) shown the downtrend of reflection coefficient for increasing frequency (Fig.7), we expect that prototype 4 will well-behave beyond 150GHz as well.

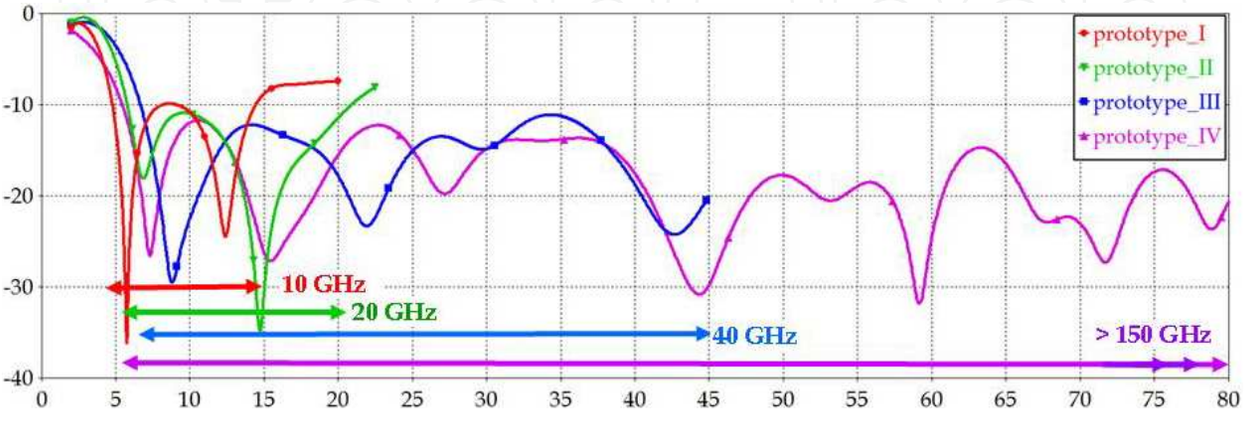

Figure 9. Impedance bandwidth of the developed prototypes. Ordinate: magnitude of the reflection coefficient [dB]; Abscissa: frequency [GHz].

Parameter (mm)	IRCTR developed prototypes			
	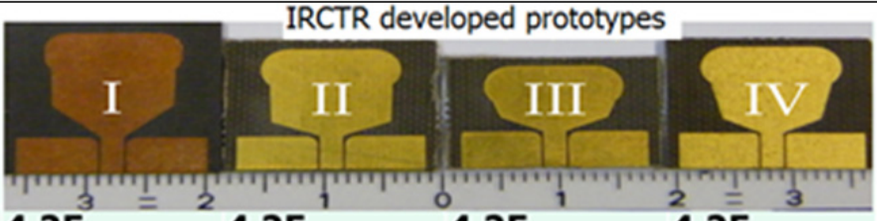			
	I	II	III	IV
L_F	4.25	4.25	4.25	4.25
R_F	0.5	0.5	0.5	0.5
W_{GND}	6.86	6.86	6.86	6.86
W_S	2	2	2	2
W_G	0.14	0.14	0.14	0.14
L_T	3.64	1.64	1.64	1.64
W_T	10.2	10.2	9.2 A	8.5 B
L_{R1}	4.33	4.33	4.33	4.33
L_{R2}	4.335	4.335	1.835 B	4.335 A
W_R	10.5	10.5	10.5	10.5
W_C	7	7	7	7.2 C
R	2.5	2.5	2.5	2.5
BW (GHz)	4-14	5-25	6.5-45	5-150

Table 2. Parameters of the prototypes; the alphabetical order A, B, C indicates the priority-order of parameters in the SVO process.

5. Design and fabrication

5.1. Design

All prototypes depicted in Fig.4, with their design dimensions listed in table.2, have been fabricated on Duroid RT 5880 high frequency laminate with substrate height h=0.787mm, copper cladding thickness t=17μm, relative dielectric constant ε_r=2.2, electric and magnetic loss tangents are given by tan δ_E=0.0027 and tan δ_H=0, respectively. The foremost reason of choosing this material is that it could relatively afford SWB frequency range up to 77 GHz (Huang et al., 2008, p.64). Other reasons are assessments related to temperature, moisture, corrosion and stability, which were investigated in details by (Brown et al., 1980).

5.2. Feed elongation

Since the dimension of the SMA connector's flange is considerably large in comparison with the antenna dimension (see Fig.10a), this comparable size exerts a huge impact on the antenna's electromagnetic-properties in particularly to the transmission, scattering and

radiation mechanism. In order to reduce this obstruction and to measure the antenna's scattering parameters and radiation patterns adequately, it is necessary to elongate the antenna as show in Fig. 10b. To back up the advocating of this elongation, we exploited the facts that the co planar waveguide has negligible radiation, low-loss and constant effective dielectric constant in rather wide range of application from DC to above 50GHz. we decided to elongate the CPW feed L_F to 40mm, and carried out numerical simulations of the same SWB radiators with short and long feed. The magnitudes of the reflection coefficient are compared and plotted in Fig.10c. As expected, the numerical results exposed a negligible differences as theoretically has predicted (Simons, 2001, p.240). Note that these theoretical properties (negligible radiation and low-loss) were also experimentally consolidated by (Tanyer et al, op cit.).

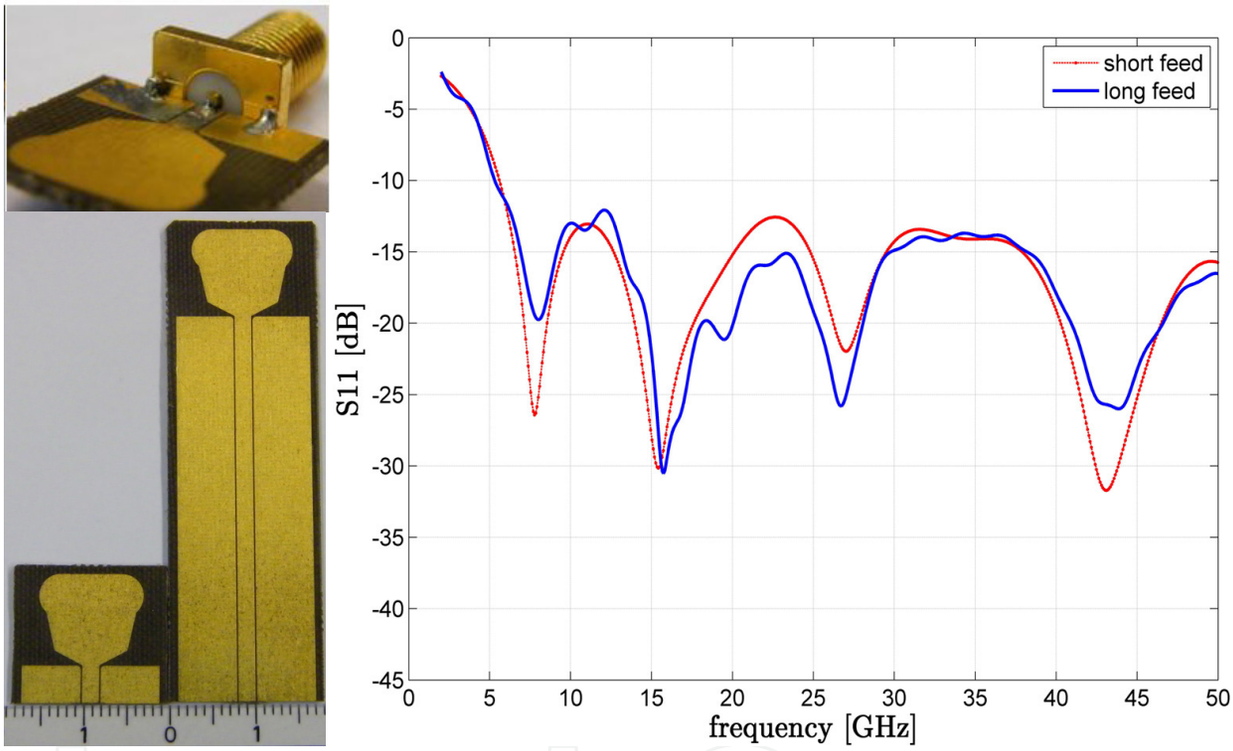

Figure 10. Conceptual demonstration for advocating of CPW feed elongation, a) radiator with SMA connector, b) radiators with short and elongated feed, b) simulated reflection coefficient magnitudes of antenna with short and long feed.

6. Measurements

6.1. Reflection coefficient

The prototype 4 is measured with the Agilent E8364B PNA vector network analyzer, the electronic calibration kit N4693A 2-port ECal-module was used for full-range calibration of the PNA (50GHz).

The reflection coefficient magnitude of prototype 4 is measured and shown in fig. 11, the measurement agreed well with predicted value. Small deviation as frequency higher than 26

GHz, this defect is inherently caused by the failure of the 3.5mm SMA-connector, whose HF-range is cataloged as 18GHz max. The result indicated that the prototype 4 is a SWB-radiator because its measured ratio-bandwidth B_R is certainly greater than 10:1.

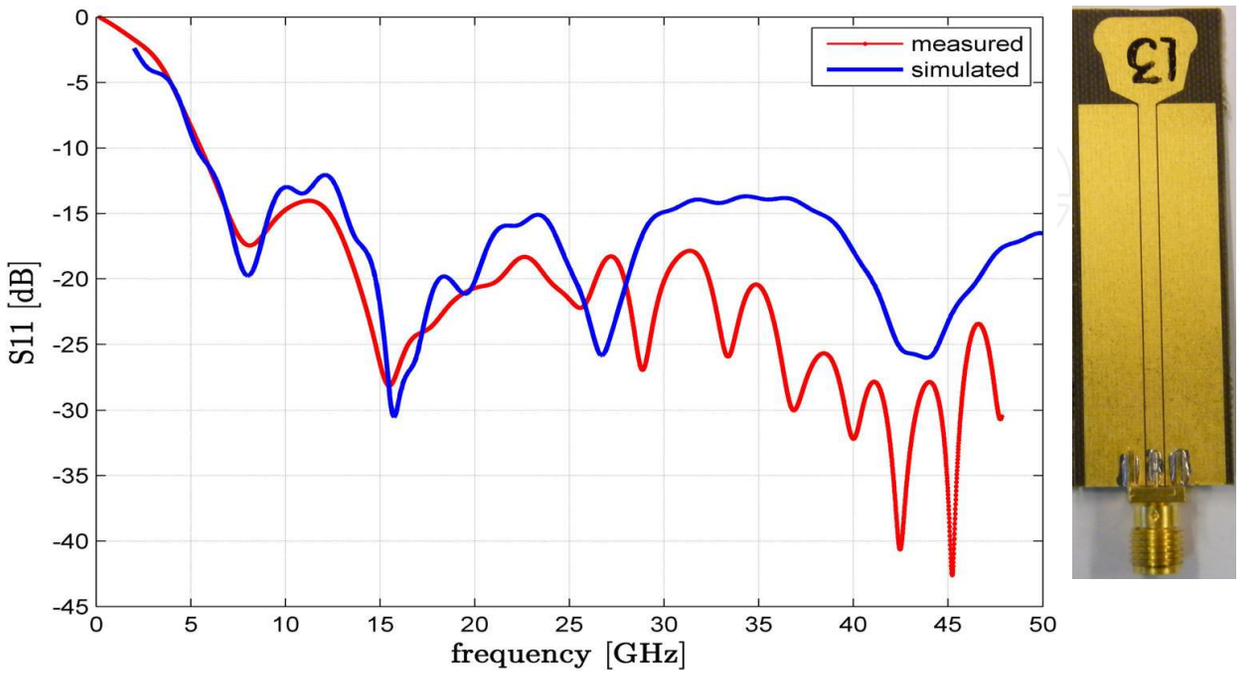

Figure 11. SWB-performance: simulated and measured results.

6.2. Far-field radiation patterns

The far field radiation patterns are measured in the Delft University Chamber for Antenna Test (DUCAT); the anechoic chamber DUCAT (Fig.12a) is fully screened, its walls, floor and ceiling are shielded with quality copper plate of 0.4 mm thick. All these aimed to create a Faraday cage of internal dimension of 6 x 3.5 x 3.5 m3, which will prevent any external signal from entering the chamber and interfering with the measurements. The shielding of the chamber is for frequencies above 2 GHz up to 18 GHz at least 120 dB all around (Ligthart, 2006). All sides are covered with Pressey PFT-18 and PFT-6 absorbers for the small walls and long walls, respectively. It is found that one side reflects less than -36 dB. All these measures were taken together in order to provide sufficient shielding from other radiation coming from high power marine radars in the nearby areas.

TX: Single polarization standard horn is used as transmitter, which can rotate in yaw-y-direction to provide V, H polarizations and all possible slant polarizations. The choice of the single polarization horn above the dual polarization one as calibrator is two-folds: 1) keeps the unwanted cross-polarization to the lowest possible level, 2) and also voids the phase center interference and keeps the phase center deviation to the lowest level.

RX: Prototype 4 is put as antenna under test (AUT) on the roll-z-rotatable column (Fig.8b). For the measurements of polarimetric components (VV, HV, VH, HH, the first letter denotes

transmission's polarization state, the second is for the reception), two measurement setups are configured, the 1st is the vertical reception setup (VRS, Fig.12c) for VV, VH and the 2nd is the horizontal reception setup (HRS, Fig.12d) for HH, HV. Combination of the two setups and the TX's two polarizations provide full polarimetric patterns of the AUT.

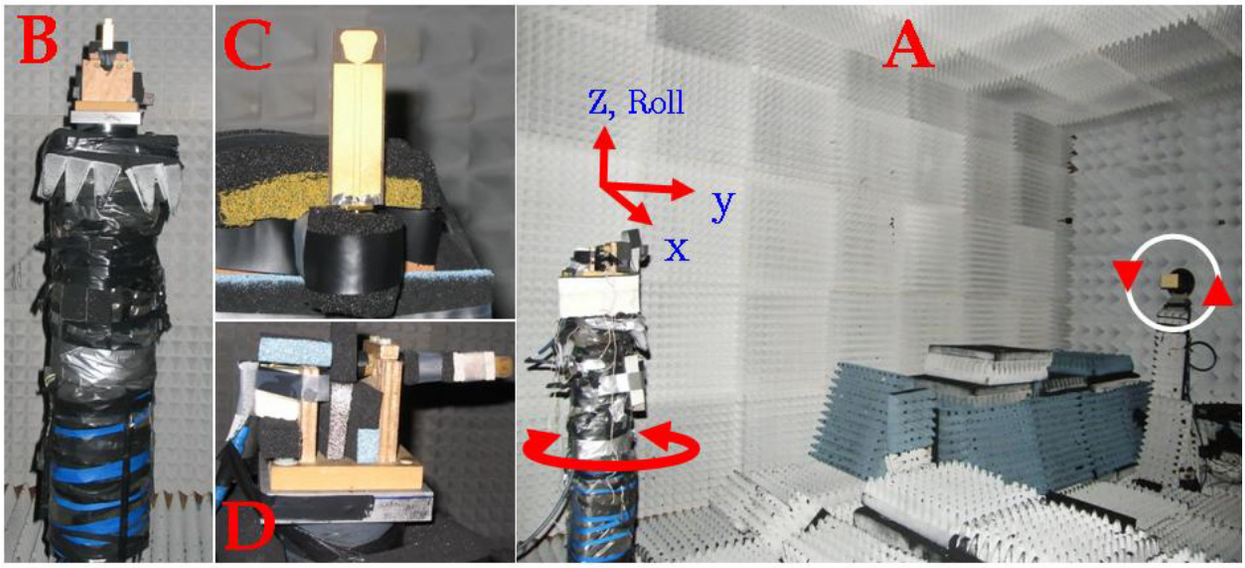

Figure 12. Patterns measurement set up: a) anechoic chamber DUCAT, b) AUT on the rotatable column, c) Vertical configuration and d) Horizontal configuration.

Calibration: the HF-ranges of the Sucoflex-cable, T-adapters and connectors used in this measurement set up all cataloged as 18GHz max, owing to this limitation, we calibrated the PNA with Agilent N4691B cal-kit (1-26GHz).

6.2.1. Co-polar VV radiation patterns

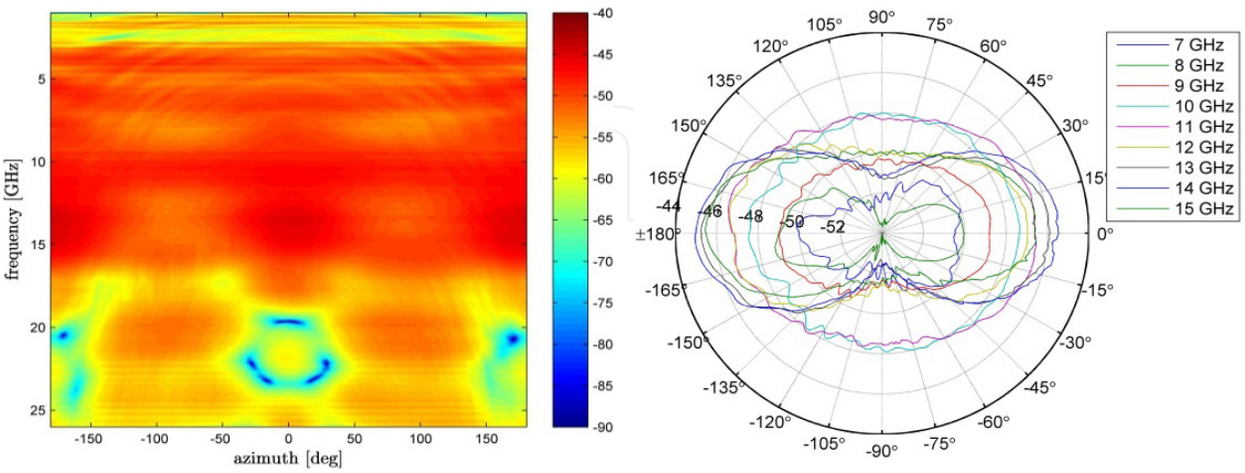

(a) (b)

Figure 13. Full-band VV co-polar measured patterns; RX: VRS; TX: zenithally oriented; a) 2D continuous patterns; b) 1D polar patterns with frequency paramaterization

6.2.2. Cx-polar HV radiation patterns

The HV cx-polar patterns are obtained with the VRS configuration in which TX-polarization in Fig.12a is 900-rotated. Plotted in Fig.14 are the HV cx-polar patterns. As expected, perfect symmetrical and repeatable patterns can be observed in full-calibrated range (1-26GHz).

Fig.14b showed the measured HV cx-polar patterns for the in-band range (7-15GHz, 1GHz increment). The patterns consolidated the repeatable symmetrical receiving/transmitting mechanism of the prototype 4. Also observed is that all EIRP are less than -65dBm, this revealed that a greater than -20dBm XPD is obtained. Note, in the yoz−plane, theoretically no cx-polar components are expected as all cross polar components cancel each other in the 0^0—180^0 and -90^0—90^0 direction. In a real case scenario, some cx-polar components are observed, their level being, nonetheless, extremely low (~ -90dBm)

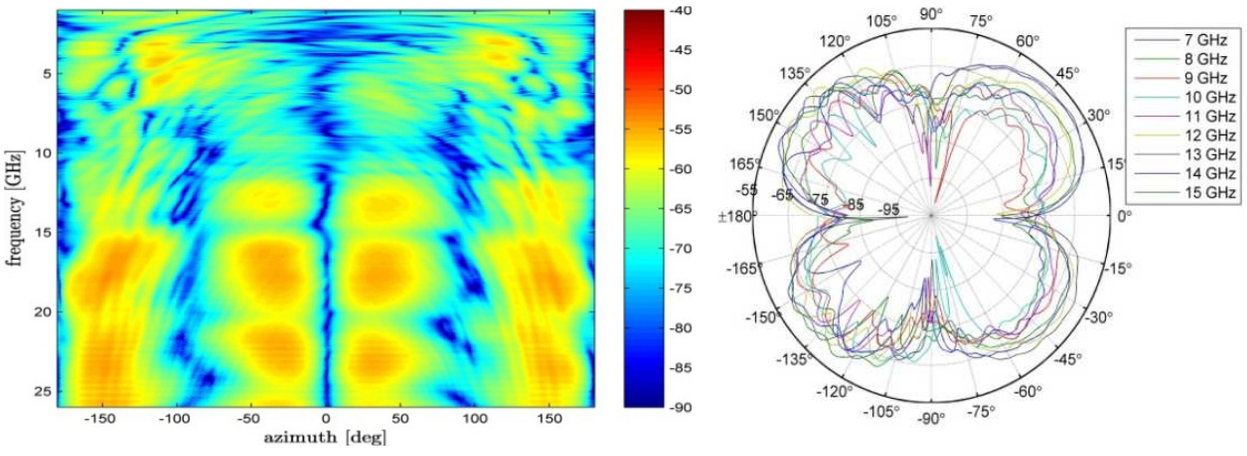

(a) (b)

Figure 14. HV cx-polar measured patterns; RX: VRS; TX: azimuthally oriented; a) 2D full-band patterns; b) Frequency parameterized 1D polar patterns

6.2.3. Co-polarized HH and Cx-polarized VH rradiation patterns

The co-polar (HH) and cx-polar (VH) radiation patterns can be acquired by the HRS with two polarization states of the TX, respectively. However, due to the mounting of the antenna (shown in Fig.12d) it was not possible to measure the backside of the antenna, thus only half of the co-polar and cx-polar patterns were measured. Owing to the frequency limitations of used components (cables, adapters, connectors, absorbents), the DUCAT anechoic chamber specifications (Ligthart, 2006, op. cit.) and the desired band the in-band range is chosen from 7-15GHz.

Fig.15a showed the measured co-polar HH in-band radiation patterns. The patterns are symmetrical and repeatable with all EIRP less than -42dBm. The measured in-band cx-polar patterns for the VH configuration are plotted in Fig.15b, all peak powers have the EIRP in the order of -60dBm. The XPD of between HH and VH of the HRS displays the same discrimination dynamic as that of VV and HV of the VRS.

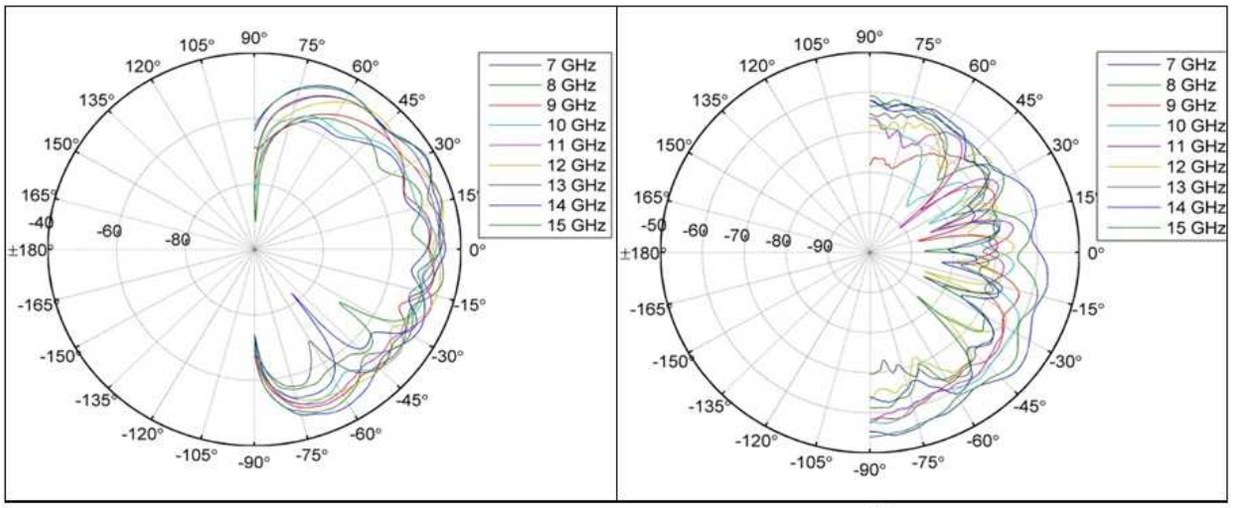

Figure 15. In-band measured patterns; a) HH co-polarized with RX: HRS and TX: azimuthally oriented; b) VH Cx-polarized with RX: VRS and TX: azimuthally oriented.

6.3. Time domain measurements

Fig.16 shows the time domain set up for measurement and evaluation of: 1) pulse deformation, 2) the omni-radiation characteristics of the AUT. The same prototype 4 are used for TX (left) and RX (right), they stand on a horizontal foam bar which situated 1.20m above the floor.

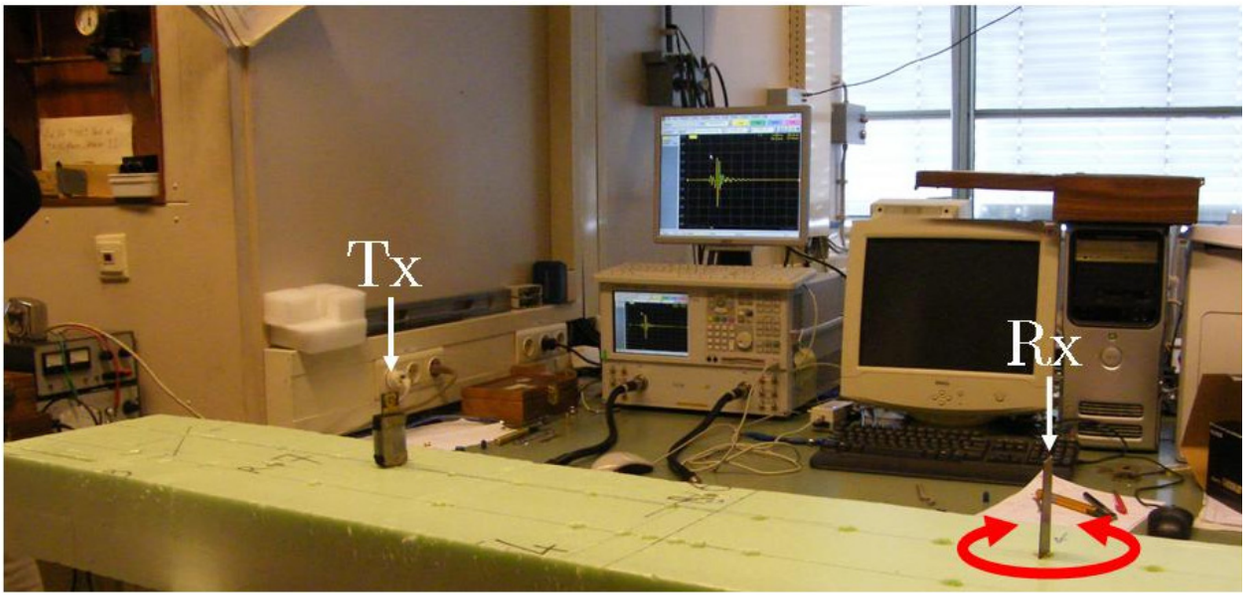

Figure 16. Time domain measurement setups, equipment: Agilent VNA E8364B; Calibration kit: Agilent N4691B, calibrated method: 2-port 3.5 mm, TRL (SOLT), 300 KHz – 26 GHz

6.3.1. Pulse measurements

Pulse spreading and deformation: Fig.17a shows the time-synchronization between the calculated transmit pulse (CTS) and the measured receive pulse (MRP) (for comparison, the CTS has been normalized, time-shifted and compared with the MRP), qualitative inspection shows that the synchronization-timing between transmitted and received pulses is very good, there is no pulse spreading took place, these measured features proved that the device is suitable for accurate ranging/sensing-applications, the small deviation at the beginning of the received pulse is due to RF-leakage (Agilent, AN1287-12, p.38), and at the end of the received pulse are from environments and late-time returns (Agilent, ibid., p.38), Note that the measurements are carried out in true EM-polluted environment as shows in fig.16, and no gating applied.

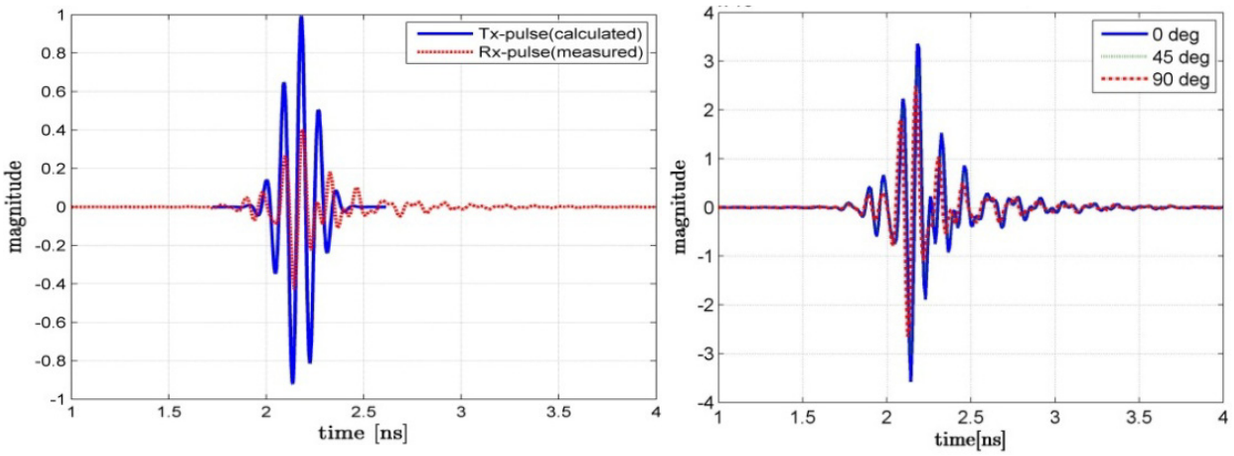

(a) (b)

Figure 17. Co-polar transmission results of VRS-configuration; a) face-to-face: calculated vs. measured; b) oblique facing: measured results with RX 0-, 45- and 90-degree rotated.

Omni-radiation characteristics: To correctly evaluate the omni-directional property of the AUT, both quantitative characteristics (spatial) and qualitative characteristics (temporal) are carried out, the spatial-properties of prototype 4 are already tested and evaluated in frequency-domain (as depicted in fig.13), and only the temporal-characteristic is left to be evaluated. To evaluated temporal-omni-radiation characteristics, three principal cuts are sufficiently represent the temporal-omni-radiation characteristics of the AUT in the time domain. Due to the editorial limitation, we report here only the most representative case (omni-directional in the azimuthal plane, i.e. co-polar VRS, which represents the most of all realistic reception scenarios). Fig.17b shows three MRPs of the measurement configuration pictured in Fig.16 with RX 0^0, 45^0, and 90^0 rotated. The results show a perfectly identical in timing, there is no time–deviation or spreading detected between the three cases. Furthermore, although the radiator is planar, it still exhibits a remarkable azimuth-independent property of 3D-symmetric radiators (for the 90^0 configuration, the projection of the receiving aperture vanished, however the prototype still able to receive 90% power as compare to the face-to-face case), this TD-measured results pertained the omni-directional property of the radiator, and this is also in agreement with, and as well consolidate the validity of the measured results carried out in the FD.

6.3.2. Transmission amplitude dispersion

To evaluate the amplitude spectral dispersion of the prototype 4, the measured time-domain transmission scattering coefficients of the three co-polar configurations (0^0, 45^0, and 90^0 configurations displayed in fig.16) were Fourier-transformed in to frequency domain. The measured magnitudes are plotted in fig.18a, the measured results show a smooth and flat amplitude distribution in the designated band, and all are lower than -42dBm.

6.3.3. Transmission phase delay and group delay

The measured phase responses of the transmission parameter for the three co-polar configurations are plotted in Fig.18b. In narrowband technology, the phase delay defined as $\tau P = -\theta/\omega$, is a metric for judging the quality of the transmission is the phase delay between the input and output signals of the system at a given frequency. In wideband technology, however, group delay is a more precise and useful measure of phase linearity of the phase response (Chen, 2007). The transmission group delays for the three above-mentioned configurations are plotted in Fig.18c. The plots show an excellent and negligible group delays in the order of sub-nanosecond, this is no surprise because the phase responses of the prototype are almost linear (fig.18b), thus the group delay, which is defined as the slope of the phase with respect to frequency $\tau G = -d\theta/d\omega$, resulted accordingly. Note: although the group delay (fig.18c) is mathematically defined as a constituent directly related to the phase, but it was impossible to visually observe directly from the phase plot (fig.18b), but well from the magnitude plot (fig.18a).

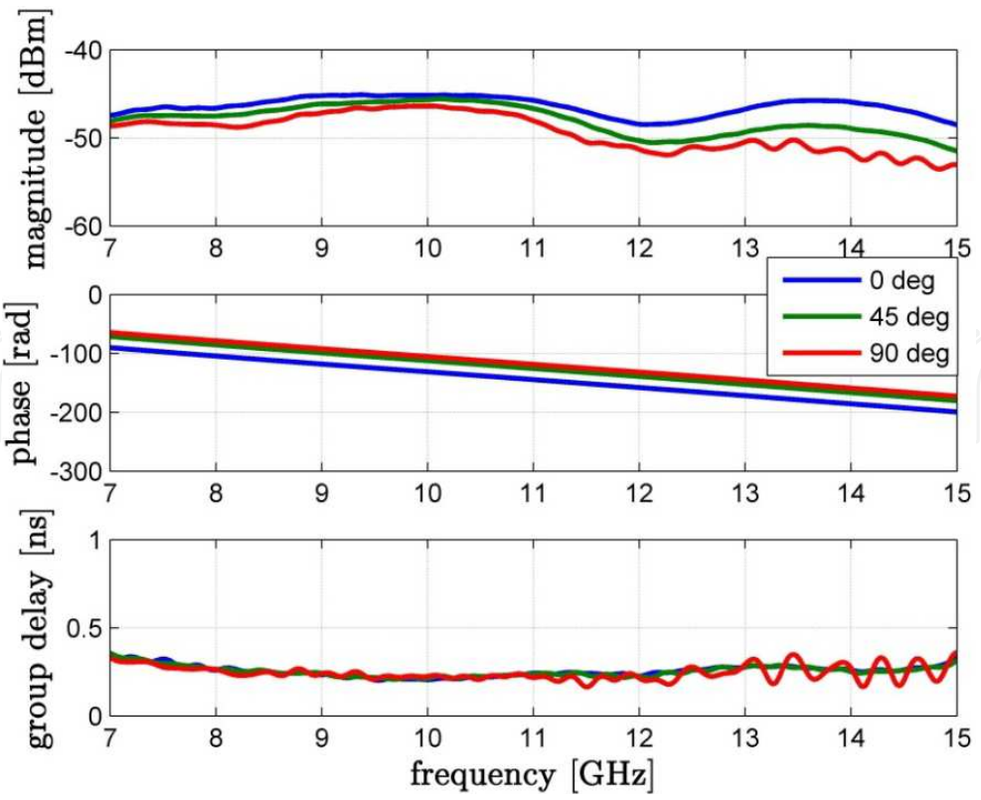

Figure 18. Measured in-band transmission coefficients a) magnitude, b) phase, c) group delay.

7. Conclusions

The intent message of this report focusses on the concept, the design methodology and the pragmatic simplification of MVO process in to a SVO one.

Distinct concepts and definitions are defused and corrected. An SWB-antenna topology with simplest structure is proposed. The single layer topology paved the way for the creating of the obtained SWB antenna architecture. The antenna architecture supported, in turn, the FSD. The introduced design methodology and conceptual concept are consolidated by the developed prototypes.

The antenna architecture provides powerful isolated-parameters to control the antenna characteristics, such as resonance-shifting, resonance matching, bandwidth broadening, diffraction reduction, and SWB pattern maintaining.

The FSD approach is introduced to obtain the required performance, whilst keeping the overall dimension of the radiator fixed, the separated sections provide engineering insights, and can be designed or optimized almost independently.

Parameter order and SVO methodology are elaborated in details, the priority and role of separable parameters are identified, and so, instead of multivariable-optimization, the optimization process can be accelerated by carry out sequence of SVOs. The proposed design, optimization procedure can possibly be used as a gauging-process for designing or optimizing similar SWB structures.

Although the prototype 4 comprised a simplest structure and shape, however superior SWB impedance bandwidth is obtained and stable SWB-patterns are uniquely preserved.

This structure, although, can be modified to obtain huge frequency bandwidth, but cannot be one-size-fit-all for gain-size requirement. However, the architecture is flexible enough for scaling up/down its dimensions to match customer's gain-size requirement.

SWB prototype is designed, fabricated and evaluated for the super wideband impasse, and could possibly be used as an alternative radiator for the sub-millimeter-wave regime.

Performances of the prototype are tested and evaluated. Good agreements between numerical predictions and measurements are obtained.

Due to editorial limits, we exclusively report here only the design methodology and conceptual approach; detailed mathematical formulation and numerical aspects related to this SWB prototype will be published in another occurrence.

Author details

D. Tran, N. Haider, S. E. Valavan, O. Yarovyi and L. P. Ligthart
International Research Centre for Telecommunication and Radar(IRCTR), Netherlands

I. E. Lager
Laboratory of Applied Mathematics, Delft University of Technology, Netherlands

A. Szilagyi
International Research Centre for Telecommunication and Radar(IRCTR), Netherlands
Military Equipment and Technologies Research Agency, Romania

Acknowledgement

The research reported in this work was effectuated with in the frame of the "Wise Band Sparse Element Array Antennas" WiSE-project, a scientific undergone financed by the Dutch Technology Foundation (Stichting Technische Wetenschapen – STW). This support is hereby gratefully acknowledged. This technological-transfer is made possible to the "Sensor

Technology Applied in Reconfigurable Systems for Sustainable Security" STARS-project thanks to the successful collaboration between two national institutions IRCTR (Netherlands), and METRA (Romania), with Thales, TNO, ASTRON and ESA as technological supervisory bodies.

8. References

Abbosh, A.M. et al. (2007), Design of a high fidelity UWB planar antenna operating in a high dielectric medium, Proceed. of the IEEE Ant. and Prop. Soc. Int. Symp. 9-15 Jun. 2007, Honolulu, USA, pp.241-244.

Balanis, C.A.(1997). Antenna theory analysis and design, Wiley Inc, 2nd ed. New York, 1997.

Bataller, M.F. et al.(2006), An overview of planar monopole antennas for UWB application, Proc Eucap 2006, Nov. Nice , France

Biscontini, B. et al.(2006), A Novel Multilayered Planar Antenna for Ultra Wide Band (UWB) Intelligent Antenna Systems, Proc. of the 22nd Ann. Rev. of Prog. in Appl. Comp. Electromagnetics ACES, March 12-16, 2006, Miami, FL; pp. 198 - 204.

Brown, D., Fiscus, T.E, Meierbachtol, C.J(1980). Results of a study using RT 5880 material for a missile radome, In: Symp. on Electromagnetic Windows, 15th, Atlanta, GA, June 18-20, Proc. (A82-2645, 11-32), Georgia Inst. of Technology, p.7-12.

Chavka, G. et al.(2006), "Radiation of ultra-wideband signals by pulse antenna" in proceeding of the Ultra-wideband and Ultra-short Impulse Signals, 18-22 September, 2006, Sevastopol, Ukraine.

Chiou, J.Y. et al.(2003), A Broad-Band CPW-Fed Strip-Loaded Square Slot Antenna, IEEE Transactions on Antennas and Propagation, Vol. 51, No. 4, April 2003, pp.719-721.

Cho, Y.J. et al.(2006), A Miniature UWB Planar Monopole Antenna With 5-GHz Band-Rejection Filter and the Time-Domain Characteristics, IEEE Trans. AP. Vol.54, No. 5, May 2006.pp-1453-1460.

Choi, S.H. et al.(2004), A new ultra-wideband antenna for UWB applications, MOTL, V.40, No.5, Mar. 2004

Choi, S.T. et al.(2009), Small printed CPW-fed triangular monopole antenna for ultra-wideband applications, IEEE Micro & Opt. Tech. Letters, Vol.51, No.5, May 2009,pp.180-182.

FCC (2002). Federal Communications Commission, FCC 02-48, ET-Docket 98-153, "*First Report and Order*", Apr. 2002.

FCC (2004), Federal Communications Commission, FCC 04-285, ET-Docket 98-153, "*Second Report and Order and Second Memorandum Opinion and Order*", Dec. 2004.

Garbaruk, M.(2008)"Design and experimental investigations of UWB microstrip and stripline antennas", Proceeding of the 17th International Conference on Microwaves, Radar and Wireless Communications, MIKON 2008.

Hayes, P.R., et al.(2007), "UWB Antenna Surrogate Design", in: Ultra-Wideband Short-Pulse Electromagnetics 8, Baum, C.E., Ed. 2007.

Huang, Y. & Boyle, K.(2008). Antennas from Theory to Practice, John Willey and Sons, Singapore, 2008, pp.64.

IEEE STD 145-1983,(1983), IEEE Standard Definitions of Terms for Antennas, New York, IEEE Press, 1983, pp.11-16.

Karoui, M.S., et al.(2010), Bandwidth Enhancement of the Square Rectangular Patch Antenna for Biotelemetry applications, International journal of information systems and telecommunication engineering, v.1, 2010, iss.1, pp.12-18.

Kraus, J. D. (1985), Antennas since Hertz and Marconi, IEEE Trans. AP-33, No. 2, Feb.1985, pp.131-137.

Kshetrimayum, R.S., Pillalamarri, R.(2008). Novel UWB printed monopole antenna with triangular tapered feed lines, IEICE Electronics express, vol.5, No. 8, pp. 242-247.

Ligthart, L.P.(2006). Antennas and propagation measurement techniques for UWB radio, Wireless personal communications, 37(3-4), pp.329-360.

Massey, P.(2007), Planar Dipole-like for Consumer Products, In: Ultra-wideband Antennas and Prop. for Comm.s, Radar and Imaging, Allen,B.(ed) Wiley 2007, pp.163-196.

Powell, J.(2004), Antenna Design for Ultra Wideband Radio, MSc. Thesis, Massachuset Inst. Of Tech. 2004,

Powell, J. (2004), Differential and Single Ended Elliptical Antennas for 3.1-10.6 GHz Ultra-wideband communications, . Proc. of the IEEE Ant. and Prop. Soc. Int. Symp. 20-25 Jun. 2004, Cambridge, MA, USA, Vol.3, pp.2935-2938.

Rahayu, Y. et al.(2008a), A Small Novel Ultra Wideband Antenna with Slotted Ground Plane, Proc. Of the Int. Conf. on Comp. and Communications. Eng. 2008, May 13-15, 2008 Kuala Lumpur, Malaysia.

Rahayu, Y., et al. (2008b). Slotted ultra wideband antenna for bandwidth enhancement, 2008, Loughborough Antennas & Propagation Conference 17-18, Mar. 2008, Loughborough, UK.

Rahim, M.K.A. & Gardner, P. (2004). The design of nine element quasi microstrip log periodic antenna, RF and microwave conference, RFM2004, 5-6 Oct. 2004, Selangor, Malaysia, pp.132–135.

Rmili, H. & Floc'h, J. M. (2008), Design and analysis of wideband double-sided printed spiral dipole antenna with capacitive coupling, Microwave and optical technology letters, Vol. 50, No.5, pp. 312-1317.

Ruengwaree, A. (2008), "Design of UWB Radar Sensors" Dissertation, 2008, Kassel univ. press GmbH, Kassel, Germany.

Shastry, P.N. et al.(2009), Planar UWB Conical Skirt Tapered Monopole Antenna; Proceed. of the 9th IEEE Wireless and Micr. Tech. Conf., WAMICON'09. 20-21 April 2009.

Schantz, H.G.(2003), Apparatus for establishing signal coupling between a signal line and an antenna structure, US pat. 6512488B2, Jan28, 2003

Schantz, H.G and Barnes, M. (2003). UWB magnetic antenna, IEEE International Symposium on Antennas and Propagation Digest, 3, 2003, pp.604-607.

Schantz, H.G. (2004). A brief history of UWB antennas, IEEE Aerospace and Electronic Systems Magazine, vol .19(4), pp.22-26, 2004.

Simons, R.N. (2001). Coplanar Waveguide Circuits, Components, and Systems, John Wiley & Sons, New York, 2001.

Tanyer-Tigrek, F.M, Tran, D., Lager, I.E., Ligthart, L.P.(2009a). CPW-fed Quasi–Magnetic Printed Antenna for Ultra-Wideband Application, IEEE Antennas and Propagation Magazine, Vol.51, No.2, April 2009, 1, pp.61-70.

Tanyer-Tigrek, F.M, Tran, D., Lager, I.E., Ligthart, L.P.(2009b). Over 150% bandwidth, quasi-magnetic printed antennas, Antennas and Prop. Soc. Int. Symp. APS2009.

Tanyer-Tigrek, F. M.(2010). Printed antenna elements with attested ultra wideband array capability, dissertation, ISBN-978-90-9024664-2, 2010, p.113-135.

Thor, R.C. (1962). A Large Time-Bandwidth Product Pulse-Compression Technique, *IRE Transaction on military electronics*, Vol. MIl-6, No.2, Apr. 1962, pp.169-173.

Tourette, S., Fortino, N., Kossiavas, G.(2006). Compact UWB printed antennas for low frequency applications matched to different transmission lines, Microwave and optical technology letters, Vol. 49, No.6, pp.1282-1287.

Tran, D., et al. (2007). A Novel CPW-fed Optimized UWB printed Antenna, Proc of the 10th
European conference on wireless technology, pp.40-43, Munich, Germany, Oct.8-10, 2007.

Tran, D.P., Coman, C.I., Tanyer-Tigrek, F.M., Szilagyi, A., Simeoni, M., Lager, I.E., Ligthart, L.P. & van Genderen, P.(2010). The relativity of bandwidth – the pursuit of truly ultra wideband radiators, In: Antennas for Ubiquitous Radio Services in a Wireless Information Society, Lager, I.E (Ed.), pp.55-74, IOS Press, 2010, Amsterdam.

Welch, T.B,et al. (2002); "The effects of the human body on UWB signal propagation in an indoor environment", Selected Areas in Communications, IEEE Journal on; 2002

Wilson, J. M (2002). Ultra-wideband a disruptive RF technology?, Intel Research and Development, Version 1.3, Sept. 10, 2002.

Valderas, D., et al., " Ultrawideband Antennas: Design and Applications", Imperial College Press, Covent Garden, London WC2H 9HE, 2011.

Xiao, J.X. et al. (2009), A novel UWB critical slot antenna with band-notched characteristics, J. of Electromagn. Wav. and Appl., Vol. 23, 2009, pp.1377–1384.

Yeo, Y. et al.(2004), Wideband slot antennas for wireless communications, IEE Proc. Microw. Antennas Propag., Vol. 151, No. 4, Aug. 2004, pp.351-355.

Ying, C. et al., An LTCC planar ultra-wideband antenna, Microw. and Opt. Tech. Letters, Vol.21, No,3, Aug.5, 2004, pp.220-222.

Zhang, et al.,(2009), Design of CPW-Fed monopole UWB antenna with a novel notched ground, Microwave and optical technology letters, Vol. 51, No.1, pp. 88-91.